

Article

The ExoMol Atlas of Molecular Opacities

Jonathan Tennyson *  and Sergei N. Yurchenko 

Department of Physics and Astronomy, University College London, London WC1E 6BT, UK;
s.yurchenko@ucl.ac.uk

* Correspondence: j.tennyson@ucl.ac.uk

Received: 25 February 2018; Accepted: 4 May 2018; Published: 10 May 2018



Abstract: The ExoMol project is dedicated to providing molecular line lists for exoplanet and other hot atmospheres. The ExoMol procedure uses a mixture of ab initio calculations and available laboratory data. The actual line lists are generated using variational nuclear motion calculations. These line lists form the input for opacity models for cool stars and brown dwarfs as well as for radiative transport models involving exoplanets. This paper is a collection of molecular opacities for 52 molecules (130 isotopologues) at two reference temperatures, 300 K and 2000 K, using line lists from the ExoMol database. So far, ExoMol line lists have been generated for about 30 key molecular species. Other line lists are taken from external sources or from our work predating the ExoMol project. An overview of the line lists generated by ExoMol thus far is presented and used to evaluate further molecular data needs. Other line lists are also considered. The requirement for completeness within a line list is emphasized and needs for further line lists discussed.

Keywords: exoplanets; brown stars; cool stars; opacity; molecular spectra; ExoMol

1. Introduction

Molecular opacities dictate the atmospheric properties and evolution of a whole range of cool stars and all brown dwarfs. They are also important for the radiative transport properties of exoplanets. Even for a relatively simple molecule, the opacity function is generally complicated as it varies strongly with both wavelength and temperature. This is because molecules interact with light via a variety of different motions, namely rotational, vibrational and electronic, and the close-spacing of the energy levels leads to strong temperature dependence related to the thermal occupancy of the levels.

Molecular opacity functions, such as the ones provided by Sharp and Burrows [1], require very extensive input in the form of temperature-dependent spectroscopic data for atoms and molecules. At room temperature, the HITRAN database [2] provides comprehensive and validated spectroscopic parameters for molecules found in the Earth's atmosphere and some other species. However, the complexity of molecular spectra increases rapidly with temperature and data from HITRAN and can only be used with extreme caution at higher temperatures [3]. The HITEMP database [4] is a HITRAN-style database designed to work at higher temperatures. However, HITEMP only contains spectroscopic line lists for five molecules and there are improved line lists available for each of these species, namely: H₂O [5], CO₂ [6,7], CO [8], NO [9], and OH [10]. The opacity of all of these species are discussed further below.

The need for extensive, high temperature spectroscopic data on molecules, many of whom do not occur in the Earth's atmosphere, has led to a number of systematic efforts to generate the molecular line lists required [7,11–16]. In particular, a number of groups have been progressively generating line lists for key molecules. These includes the TheoReTS [16] group (Reims/Tomsk), the NASA Ames team and our own ExoMol activity based in University College London, all of which used similar theoretical procedures discussed below, and an experimental initiative led by Bernath [14]. These activities have

been significantly enhanced by the discovery of exoplanets and the requirement of extensive line lists to be used in exoplanet models and characterization [17,18].

As molecular line lists are extended, complicated and have a strong temperature dependence, it can be hard to understand a priori spectral regions where they show significant absorption. This work aims to summarize the absorption by the key molecular species required for cool stars, brown dwarfs and exoplanets. Many of the line lists used are taken from those computed by the Exomol project, but these are augmented by lists taken from other sources to give a comprehensive set, or atlas, of absorbing species.

In this work, we present a collection (atlas) of molecular opacities for 52 molecules (130 isotopologues) generated using line lists from the ExoMol database. The opacities are presented in the form of cross sections for two reference temperatures, 300 K and 2000 K using the Doppler (zero-pressure) broadening. The goal of this atlas is to present in a simple, visual form an overview of spectroscopic coverage, main spectroscopic signatures as well as temperature dependence of the molecular opacities relevant for atmospheric studies of hot exoplanets and stars.

2. Methodology

The general methodology used by the ExoMol project is very similar to that used by both the TheoReTS and NASA Ames group for producing molecular line lists. It has been well-described elsewhere [19,20] and below we will discuss only general considerations.

Our technique involves the following general steps: (1) computing accurate ab initio potential energy and dipole surface moment surfaces, (2) improving the potential energy surface (PES) using available high-resolution spectroscopic data and (3) generating a comprehensive line list using the improved PES, ab initio dipole moment surface (DMS) and an appropriate variational nuclear motion program [21–23]. Development of these program specifically for opacity calculations has been discussed by us elsewhere [24].

Performing such calculations is always a trade-off between completeness and accuracy. A complete line list should contain information on possible transitions at all wavelengths and at all temperatures. An accurate one should reproduce line positions and transition probabilities to the high standards of laboratory high resolution spectroscopy. In practice, for most systems, it is hard if not impossible to achieve both of these goals simultaneously so compromises have to be made. Experience shows that completeness is essential [25] while accuracy is something to strive for and, of course, is essential for high resolution spectroscopic studies [26].

Starting from an ab initio PES, there are three ways of improving the accuracy of the line positions. The first method is to fit the potential to measured transitions frequencies, empirical energies or a mixture of both. This is now a standard technique that is widely employed. It is capable of giving very good results [27] if in most cases not actual experimental accuracy. The second technique is to adjust the vibrational band origins during the calculation. This technique works only if the rotation–vibration basis used is a simple product between vibrational and rotational functions. A basis in this form is used by the polyatomic nuclear motion program TROVE [23] and the vibrational basis is contracted by performing an initial rotationless ($J = 0$) calculations. At this stage, the band origins can be shifted to their empirical value [28]. Finally, the ExoMol data structure [29] presents a line list as a states file with energy levels and associated quantum numbers and a highly compact transitions file of Einstein A coefficients. This structure therefore allows computed energy levels to be replaced with empirical ones after the calculation is complete; indeed, this can be done some time after the line list is computed if new empirical data becomes available [30]. This allows many transition frequencies to be generated with experimental accuracy, including ones that have not actually been measured.

To provide lists of accurate empirical energy levels, Furtenbacher et al. [31,32] developed the measured active rotation vibration energy level procedure (MARVEL). Table 1 gives a summary of molecules of astronomical importance for which the MARVEL procedure has been applied. Overviews of this methodology can be found elsewhere [33,34].

Table 1. Summary of MARVEL analyses performed for astronomically important molecules.

Molecule	N_{iso}	N_{trans}	N_E	Reference(s)
H ₂ O	9	182,156	18,486	[35–38]
H ₃ ⁺	3	1410	911	[39,40]
NH ₃	1	28,530	4961	[41]
C ₂	1	23,343	5699	[42]
TiO	1	48,590	10,564	[43]
HCCH	1	37,813	11,213	[44]
SO ₂	3	40,269	15,130	[45]
H ₂ S	1	39,267	7651	[46]
ZrO	1	21,195	8329	[47]

N_{iso} : Number of isotopologues considered; N_{trans} : Number of transitions validated for the main isotopologue; N_E : Number of energy levels given for the main isotopologue.

The line lists generated by the methods discussed above form the input to opacity calculations. To judge the potential influence of each molecule on the opacity, one can generate cross sections as a function of wavelength and temperature. As several of the line lists considered contain many billions of lines (see Table 2), calculating cross sections can be computationally expensive. For this reason, we have developed a highly optimized program ExoCross [48], which generates wavelength-dependent cross sections as function of temperature and pressure. Here, we use ExoCross to systematically generate cross sections for the key species that are important for opacities of cool stars, brown dwarfs and exoplanets.

In generating these cross sections, we consider the main (parent) isotopologue of each species, which is taken as being in 100 % abundance. For simplicity, we use a Doppler profile on a wavenumber grid of 1 cm⁻¹. The cross sections have been generated using the methodology by Hill et al. [49]. The cross sections can be also obtained at higher resolutions (up to 0.01 cm⁻¹) using the cross sections App at www.exomol.com.

Cross sections were generated at two standard temperatures of 300 K and 2000 K except when the molecule is expected to be entirely in the condensed phase at 300 K. For a few, key strongly bound species, we also consider the cross section at 5000 K, which is near the upper limit of the temperature where molecules make a contribution to opacities.

3. Results

Table 2 summarises the molecules for which line lists have been provided as part of the ExoMol project. Sources for line lists of other key species are given in Table 3. Data for all these species, including cross sections, are available on the ExoMol website.

Figures 1–15 display temperature-dependent cross sections for each of these species. For all molecules except water, only results for the major (parent) isotopologue are given. As specified in Table 2, many ExoMol line lists also consider isotopically substituted species. In most cases, isotopic substitution leads to shifts in spectroscopic features that are observable at medium to high resolution but result in no fundamental change in structure of the spectrum. The exception is where this substitution leads to breaking of the symmetry, which can lead to new features due to changes in the way the Pauli principle applies, examples here include ¹²C¹²C to ¹²C¹³C, and changes in vibrational structure such as those encountered on moving from H₂O to HDO.

Table 2. Datasets created by the ExoMol project and included in the ExoMol database [50].

Paper	Molecule	N_{iso}	T_{max}	N_{elec}	N_{lines}	DSName	Reference
I	BeH	1	2000	1	16,400	Yadin	[51]
I	MgH	3	2000	1	10,354	Yadin	[51]
I	CaH	1	2000	1	15,278	Yadin	[51]
II	SiO	5	9000	1	254,675	EJBT	[52]
III	HCN/HNC	1	4000	1	399,000,000	Harris	[30]
IV	CH ₄	1	1500	1	9,819,605,160	YT10to10	[53]
V	NaCl	2	3000	1	702,271	Barton	[54]
V	KCl	4	3000	1	1,326,765	Barton	[54]
VI	PN	2	5000	1	142,512	YYLT	[55]
VII	PH ₃	1	1500	1	16,803,703,395	SAITY	[56]
VIII	H ₂ CO	1	1500	1	10,000,000,000	AYTY	[57]
IX	AlO	4	8000	3	4,945,580	ATP	[58]
X	NaH	2	7000	2	79,898	Rivlin	[59]
XI	HNO ₃	1	500	1	6,722,136,109	AlJS	[60]
XII	CS	8	3000	1	548,312	JnK	[61]
XIII	CaO	1	5000	5	21,279,299	VBATHY	[62]
XIV	SO ₂	1	2000	1	1,300,000,000	ExoAmes	[63]
XV	H ₂ O ₂	1	1250	1	20,000,000,000	APTY	[64]
XIV	H ₂ S	1	2000	1	115,530,3730	AYT2	[65]
XV	SO ₃	1	800	1	21,000,000,000	UYT2	[66]
XVI	VO	1	2000	13	277,131,624	VOMYT	[67]
XIX	H ₂ ^{17,18} O	2	3000	1	519,461,789	HotWat78	[68]
XX	H ₃ ⁺	1	3000	1	11,500,000,000	MiZATeP	[69]
XXI	NO	6	5000	2	2,281,042	NOName	[9]
XXII	SiH ₄	1	1200	1	62,690,449,078	OY2T	[70]
XXIII	PO	1	5000	1	2,096,289	POPS	[71]
XXIII	PS	1	5000	3	30,394,544	POPS	[71]
XXIV	SiH	4	5000	3	1,724,841	SiGHTLY	[72]
XXV	SiS	12	5000	1	91,715	UCTY	[73]
XXVI	HS	6	5000	1	219,463	SNaSH	[74]
XXVI	NS	6	5000	1	3,479,067	SNaSH	[74]
XXVII	C ₂ H ₄	1	700	1	49,841,085,051	MaYTY	[75]
XXVIII	AlH	3	5000	3	40,000	AlHambra	[76]
XXIX	CH ₃ Cl	2	1200	1	166,279,593,333	OYT	[75]
XXX	H ₂ ¹⁶ O	1	5000	1	1,500,000,000	Pokazatel	[5]
XXXI	C ₂	3	5000	8	6,080,920	8State	[77]
XXXII	MgO	3	5000	4	22,579,054	LiPTY	[78]

N_{iso} : Number of isotopologues considered; T_{max} : Maximum temperature for which the line list is complete; N_{elec} : Number of electronic states considered; N_{lines} : Number of lines, value is for the main isotopologue; DSName: Name of line list and of data set in ExoMol database [50].

For most species, absorption cross sections are plotted at two temperatures: 300 K and 2000 K. Exceptions are where the species is unlikely to have significant vapor pressure at 300 K, when this curve has been omitted, or when the species unlikely to survive at 2000 K, in which case an appropriate, lower temperature is used. The figures are grouped according to whether the line lists concerned cover the infrared only (wavenumbers below 12,000 cm⁻¹), extend into the visible (wavenumbers below 20,000 cm⁻¹) or cover the near ultraviolet (wavenumbers below 35,000 cm⁻¹). Beyond that, the figures are grouped to contain roughly similar species. Each of the figures and species are considered in turn below.

Table 3. Other molecular line lists considered. These data can also be obtained from the ExoMol website.

Molecule	N_{iso}	T_{max}	N_{elec}	N_{lines}	DSName	Reference	Methodology	
							Line Positions	Intensities
NH ₃	2	1500	1	1,138,323,351	BYTe	[79]	empirical ^a	ab initio ^a
LiH	1	12,000	1	18,982	CLT	[80]	ab initio	ab initio
ScH	1	5000	6	1,152,827	LYT	[81]	tuned ab initio	ab initio
NH	1		1	10,414	14BrBeWe	[82]	empirical	ab initio
CH	2	6000	4	54,086	14MaPIVa	[83]	empirical	ab initio
CO	9	9000	1	752,976	15LiGoRo	[8]	empirical	emp./ab initio ^b
OH	1	6000	1	45,000	16BrBeWe	[10]	empirical	ab initio
CN	1		1	195,120	14BrRaWe	[84]	empirical	ab initio
CP	1		1	28,735	14RaBrWe	[85]	empirical	ab initio
HCl	1		1	2588	11LiGoBe	[86]	empirical	ab initio
FeH	1		2	93,040	10WEReSe	[87]	empirical	ab initio
TiH	1		3	181,080	05BuDuBa	[88]	empirical	ab initio
CO ₂	13	1000	1	149,587,373	Ames-2016	[7]	empirical	ab initio
TiO	1		13	45,000,000	Schwenke	[89]	tuned ab initio	ab initio
C ₂ H ₂	1	1000	1	33,890,981	ASD-1000	[90]	effect. Hamilt. ^c	effect. dipole ^c
CrH	1		2	13,824	02BuRaBe	[91]	empirical	ab initio
CH ₃ F	1	400	1	1,391,882,159	OYKYT	[92]	ab initio	ab initio

N_{iso} : Number of isotopologues considered; T_{max} : Maximum temperature for which the line list is complete (where stated); N_{elec} : Number of electronic states considered; N_{lines} : Number of lines: value is for the main isotopologue; DSName: Name of line list and of data set in ExoMol database [50]; ^a ExoMol methodology, see text; ^b A mixture of empirical and ab initio values of the dipole moment function; ^c Empirical, based on Effective Hamiltonian and Dipole moment expansions.

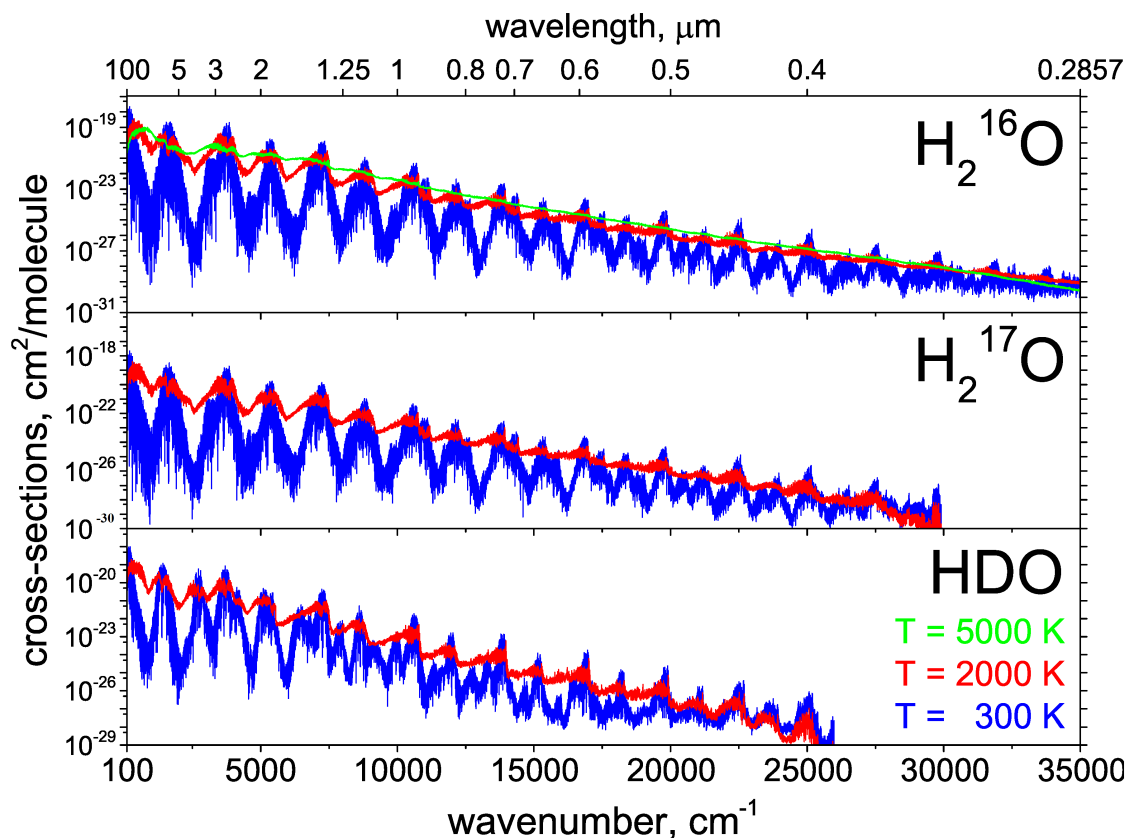


Figure 1. Cross sections for H₂¹⁶O from the POKAZATEL line list [5], H₂¹⁷O from the HotWat78 line list [68] and HDO from the VTT line list [93]. All cross sections are for 100% abundance.

H₂O: the spectrum of water (see Figure 1) is important in a whole range of astronomical objects [14] including M-dwarfs [94] and exoplanets [95]. The ExoMol line lists for H₂¹⁸O and H₂¹⁷O complement the H₂¹⁶O BT2 line list [96], which has been widely used for astronomical studies including, for instance, as the foundation of the BT-Settl cool star model atmosphere [97]. A comprehensive line list for HDO is also available [93]. In fact, we have recently updated BT2 with a new H₂¹⁶O line list known as POKAZATEL [5]. Besides greatly improving the accuracy of the previous line list, it also extends the temperature range beyond 3000 K, which BT2 was designed for. POKAZATEL has been tested against laboratory spectra recorded in flames and was found to perform very well [98]. On the scale of the figure, BT2 and POKAZATEL are very similar for temperatures below 2000 K, although the detailed line positions given by POKAZATEL are considerably more accurate (see the laboratory study by Campargue et al. [99], for example). However, at high temperatures, POKAZATEL is much more complete. What is really noticeable is how flat the water opacity becomes at high temperatures.

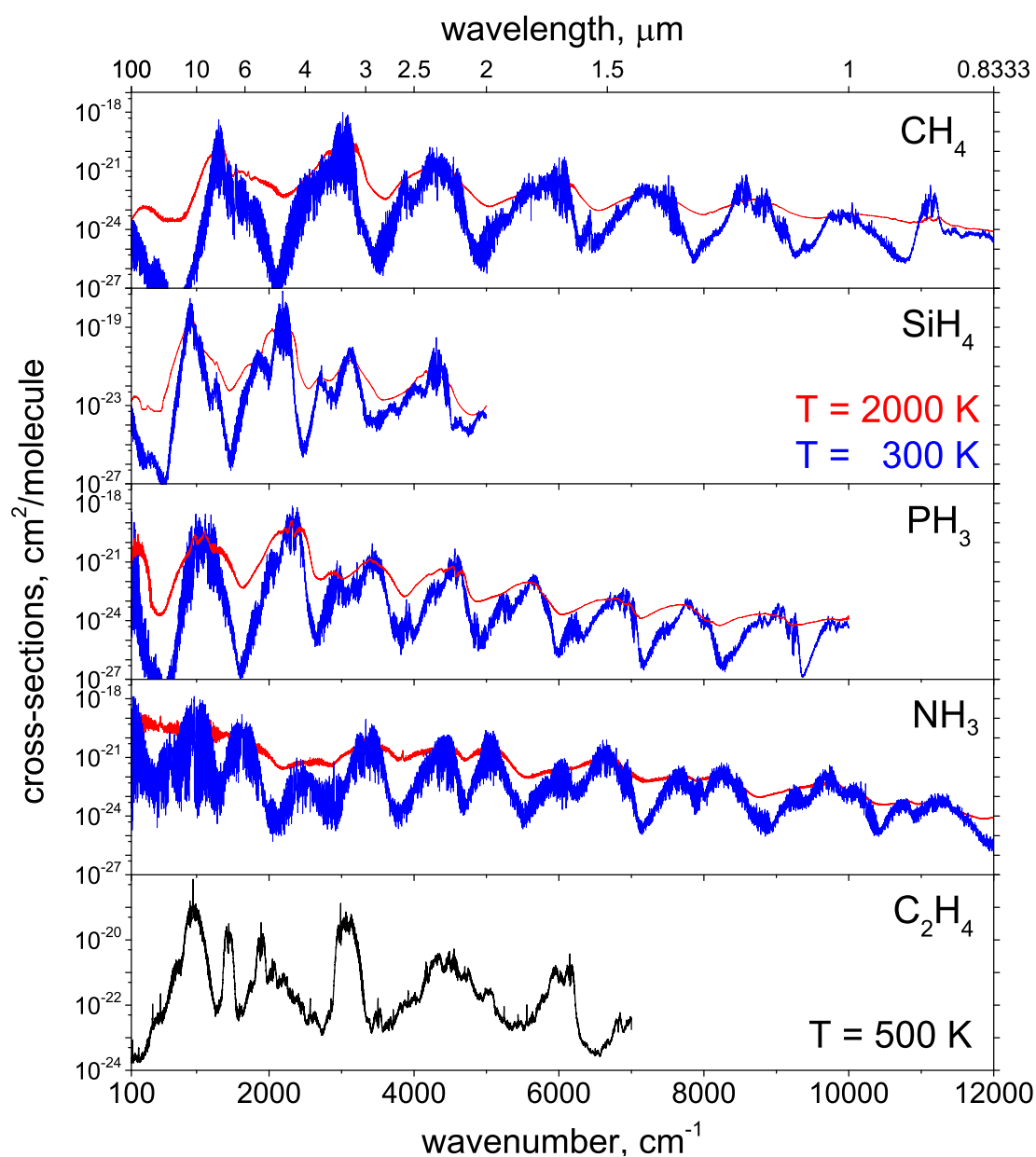


Figure 2. Cross sections generated using ExoMol line lists for methane, 10to10 line list [53], silane [72], phosphine [56], ammonia [79] and ethylene [75].

Figure 2 shows cross sections for a number of other hydrides: methane, silane, phosphine, ammonia and ethylene.

CH₄: Figure 2 shows the methane cross sections generated by the 10to10 line list, which contains almost 10^{10} transitions. Other line lists available for methane are notably the TheoReTS line list(s) [100,101], and a comprehensive experimental line list from Hargreaves et al. [102,103]. The 10to10 line list has been used to identify spectroscopic features in T-dwarfs [104]. Model calculations have shown that reproducing the atmospheric opacity of these methane-rich brown dwarfs requires the explicit consideration of many billions of transitions [25]. As the temperature range of 10to10 is limited, we have recently extended it with a new 34to10 line list, which contains 34×10^{10} transitions [105]. To make use of this line list tractable in radiative transport models, the weak lines are amalgamated into so-called super-lines [16]. The temperature coverage for the various methane line lists, which broadly agree with each other, is probably now adequate for astrophysical purposes. However, there is a need for better coverage at shorter wavelengths ($<0.85 \mu\text{m}$).

PH₃: the phosphine cross sections (see Figure 2) show a very pronounced feature about $4.5 \mu\text{m}$, which displays only weak dependence on temperature. Phosphine is a well-known component of solar system gas giants [106], and it can be anticipated that this feature will at some point be used to identify PH₃ in exoplanets.

NH₃: the spectrum of ammonia is given in Figure 2. Ammonia spectra are well known in brown dwarfs [104] and are thought to provide the key signature for coolest class of these species known as Y-dwarfs. Plotted is the BYTe line list, which is significantly less accurate than most of the other line lists considered here and is really only complete for wavenumbers below $10,000 \text{ cm}^{-1}$ and $T < 1500 \text{ K}$. A new ExoMol line list that should help resolve these issues is currently under construction. A line list for ¹⁵NH₃ is also available [107].

C₂H₄: the final spectrum given in Figure 2 is of ethylene. Only one temperature is plotted since, despite containing 60 billions line, the line list is only complete up to 700 K. However, it is likely that ethylene will decompose at higher temperatures. Although not shown here, the main features of the ethylene spectrum show an unusually small sensitivity to temperature [75]. Rey et al. [108] have also computed a far-infrared ethylene line list.

Figure 3 shows cross sections for a variety of polyatomic oxides plus hydrogen cyanide.

H₂O₂: hydrogen peroxide cross sections are given in Figure 3. It should be noted that even at room temperature the line list for H₂O₂ given by the current release of HITRAN [2] is not complete, as the strong mid-infrared absorptions are missing. This is because of the difficulty of analyzing the observed spectra in this region.

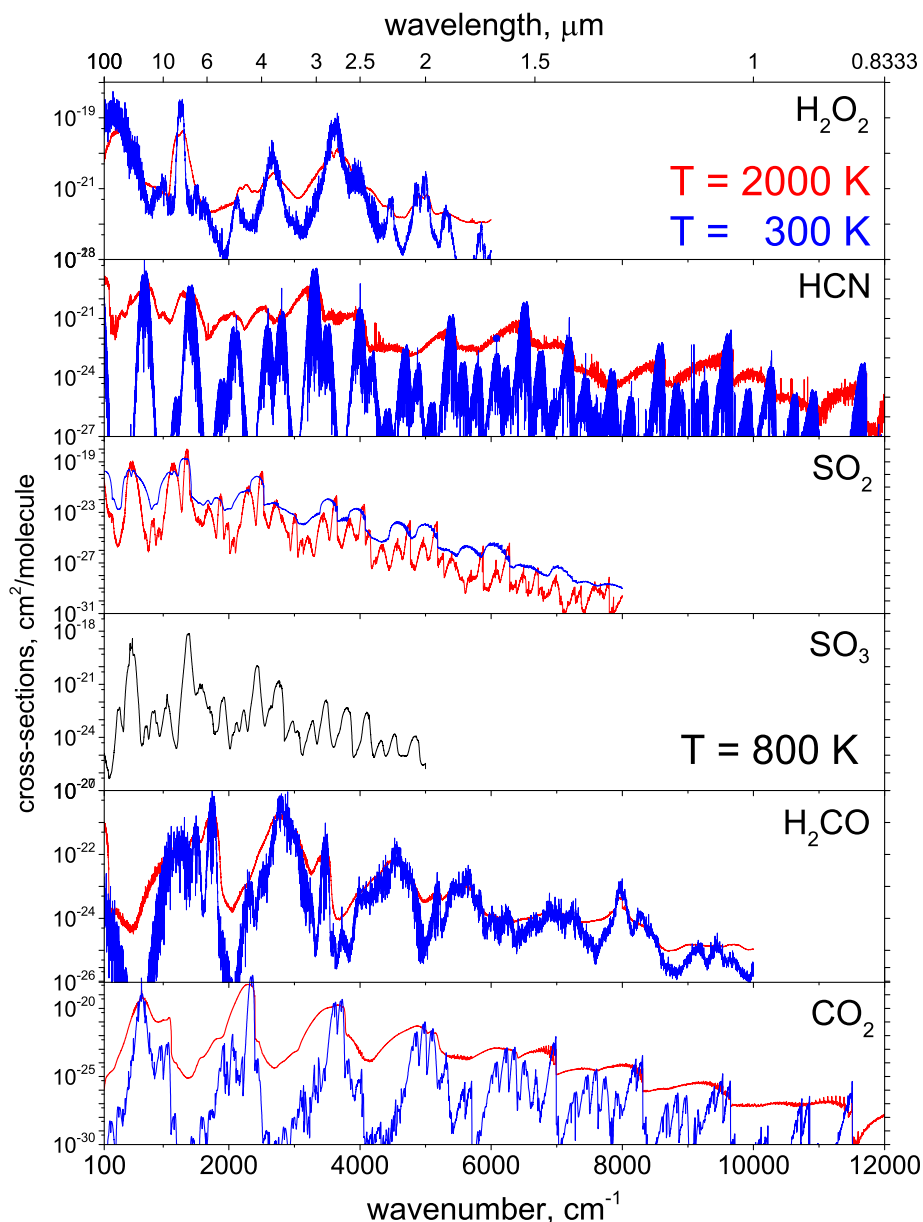


Figure 3. Cross sections for polyatomic oxides and HCN. Line lists are from ExoMol for hydrogen peroxide [109], hydrogen cyanide [30], sulfur dioxide [63], nitric acid [60] and sulfur trioxide [66]. The carbon dioxide data is taken from Ames-2016 [7].

HCN: the line list shown in Figure 3 is unusual for two reasons. First, it contains transition sets for two isomers, HCN and HNC, which are often considered to be distinct molecules and second it is not new; rather it is a reworking of earlier line lists [110,111] based on extensive compilations of empirical energy levels due to Mellau [112–114]. A similar empirically-informed line list is available for H^{13}CN [115]. The updated Harris line list was used to tentatively identify HCN in super-Earth exoplanet 55 Cancri e [116]. However, the $1.54\ \mu\text{m}$ feature used for this detection is close to a similar acetylene feature. As discussed below, there is still no good line list for hot acetylene. The opacity of HCN is particularly important for reliable models of cool carbon stars where its inclusion leads to fundamental changes in the stellar structure [117]. The ratio between HCN and HNC can provide a potential thermometer the atmospheres of cool stars [118].

SO₂: sulphur dioxide cross sections are given in Figure 3. SO₂ is thought to be an important component of oxygen-rich exoplanet atmospheres [119,120] and to have been important in both early-Earth [121] and early-Mars [122].

SO₃: sulphur trioxide cross sections are given in Figure 3. SO₃ can be hard to detect because it usually appears in conjunction with SO₂, which absorbs strongly in the same region. Interestingly, our cross sections suggest that it may be easier to distinguish SO₃ from SO₂ at higher temperatures as, while the spectrum SO₃ retains much of its structure at higher temperatures, the spectrum of SO₂ becomes increasingly flattened. The line list is only complete up to 800 K and this has been used as the upper temperature.

H₂CO: Figure 3 shows temperature dependent cross sections of formaldehyde.

CO₂: carbon dioxide cross sections given in Figure 3 are obtained from the Ames-2016 (4000 K) line list of Huang et al. [7,123], for the main isotopologue (¹²C¹⁶O₂) and covers rotational excitations up to $J = 220$. The line list is based on an empirical potential energy surface and accurate variational nuclear motion calculations. The Ames-2016 database also contains line lists for 12 other isotopologues of CO₂.

Figure 4 shows cross sections of HNO₃, CH₃Cl and C₂H₂.

HNO₃: nitric acid, whose spectrum is shown in Figure 4, is not likely to be an important source of opacity. However, its spectroscopic signature can be clearly observed in the Earth's atmosphere from space [3,124,125] and thus HNO₃ could be a possible biomarker on exoplanets. Like H₂O₂, the HITRAN data for HNO₃ is incomplete for frequencies above about 1000 cm⁻¹.

CH₃Cl: methyl chloride is also a potential biosignature in the search for life outside of the solar system [126]. ExoMol's mew line list for methyl chloride covers the two major isomers, CH₃³⁵Cl and CH₃³⁷Cl.

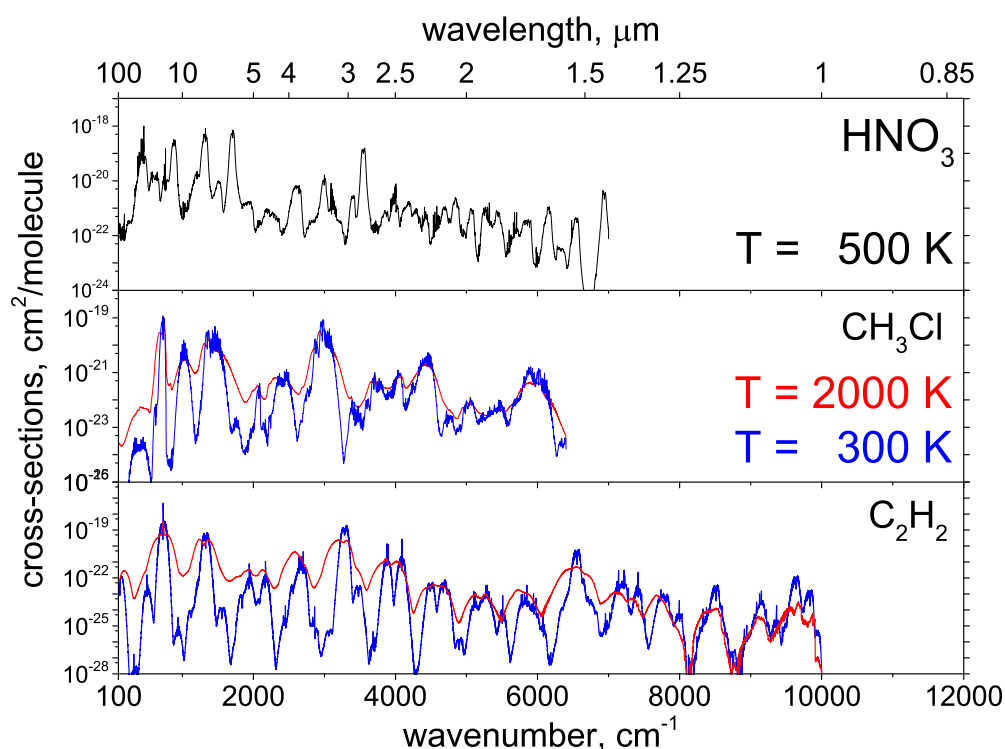


Figure 4. Cross sections obtained from ExoMol line lists for HNO₃ [60], CH₃Cl [75], and C₂H₂ [90].

C₂H₂: acetylene cross sections given in Figure 4 are generated using the ASD-1000 database [90]. ASD-1000 was generated using an Effective Hamiltonian and contains about 34,000,000 lines. This would appear to be too few lines for the line list to be complete at elevated temperatures as normally, hot line lists

for tetratomics contain billions of transitions in order to be complete for high temperatures. A variational acetylene line list is currently under construction as part of the ExoMol project.

H₂S: Figure 5 shows that hydrogen sulphide has a rather unusual spectrum. Transitions involving the vibrational fundamentals are anomalously weak [127] for this system, which shifts the peak of the vibration–rotation spectrum to shorter wavelengths than is usual: the figure shows that the strongest vibration band is an overtone lying in the 2.5 μm region.

Figure 6 gives cross sections for NS as well as the alkaline earth monohydrides MgH and CaH. Together with BeH, MgH and CaH were the first set of species considered by ExoMol. These ExoMol line lists only contain pure rotation and rotation–vibration transitions within the $X^2\Sigma^+$ electronic ground states for each of these species.

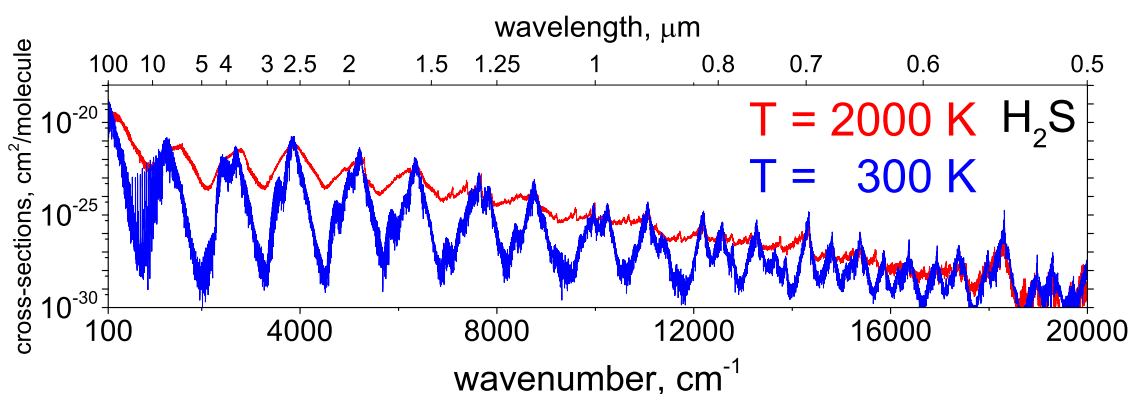


Figure 5. Cross sections for hydrogen sulfide generated using the ExoMol line list for H₂S [65].

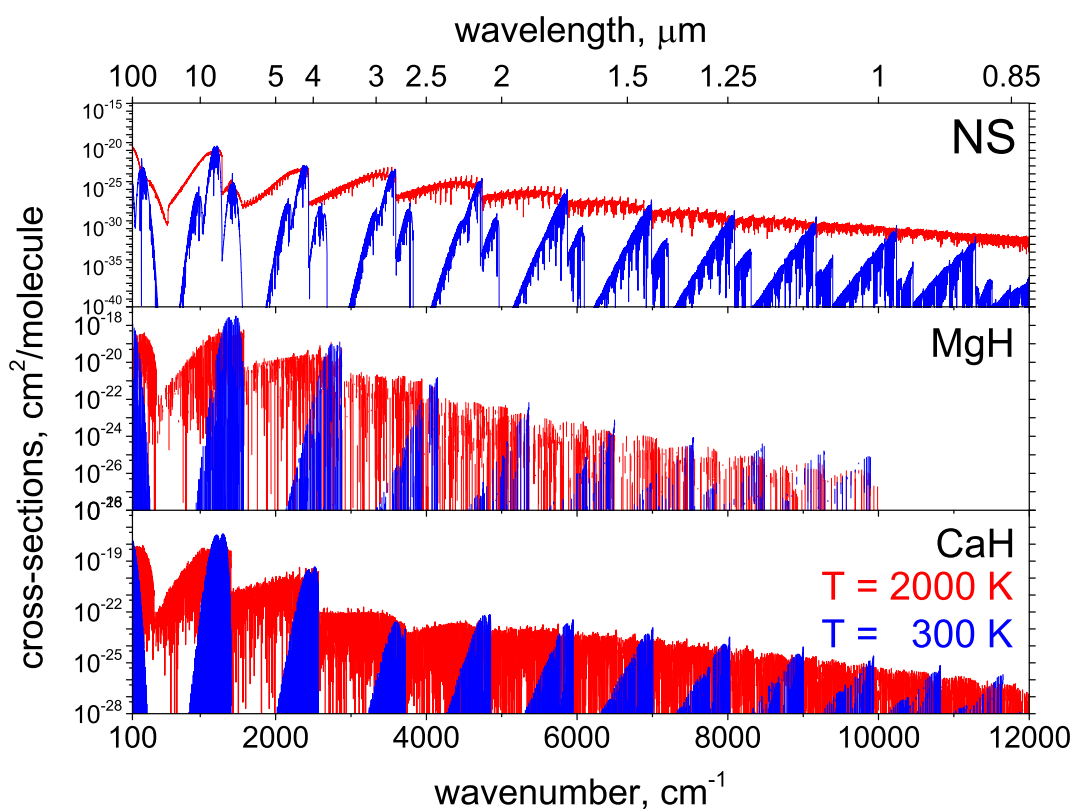


Figure 6. Cross sections for alkaline earth monohydrides MgH and CaH from the Yadin ExoMol line lists [51] and NS from the SNaSH line list [74].

NS: NS is one of the first ten diatomic molecules to be detected in space [128,129].

MgH: the $A^2\Pi-X^2\Sigma^+$ band is also important for magnesium monohydride as, in particular, its use of major importance for establishing isotopic abundances of Mg in stars [130–134]. Weck et al. [13] constructed a purely ab initio line list, which covers this band but is of limited accuracy. More recently, experimentally-driven studies [135,136] have sought to remedy this problem.

CaH: A $^2\Pi-X^2\Sigma^+$ band is also important in cool stars and brown dwarfs [137].

Figure 7 shows cross sections covering electronic spectra of three diatomic monohydrides, BeH, AlH and CH.

BeH: Darby-Lewis et al. [138] have recently developed a new model for beryllium monohydride, which both improves (marginally) on the earlier Yadin line list [51] and, more significantly, includes a treatment of the $A^2\Pi-X^2\Sigma^+$ band. This band has been observed in sunspot [139], but the motivation for extending the line list was actually fusion plasmas where the use of Be walls has led to the observation of A–X emissions in the plasma [140]. Darby-Lewis et al. demonstrate that their new line list gives excellent reproduction of emission spectra of both BeH and BeD, as well as predictions for the spectrum of BeT, which is important for fusion studies.

AlH: it is known to be present in sunspots through lines in its $A^1\Pi-X^1\Sigma^+$ electronic band which lie in the blue [141]; AlH was also recently detected around Mira-variable o Ceti by Kaminski et al. [142]. The ExoMol line list for AlH contains these electronic transitions as well as ground state lines.

CH: an extensive, empirical line list is available for CH due to Masseron et al. [83]. This line list covers transitions within the $X^2\Pi$ electronic ground state as well as rovibronic transitions within the $A^2\Delta-X^2\Pi$, $B^2\Sigma^- - X^2\Pi$ and $C^2\Sigma^+ - X^2\Pi$ bands. Masseron et al. [83] also provide a line list for ^{13}CH .

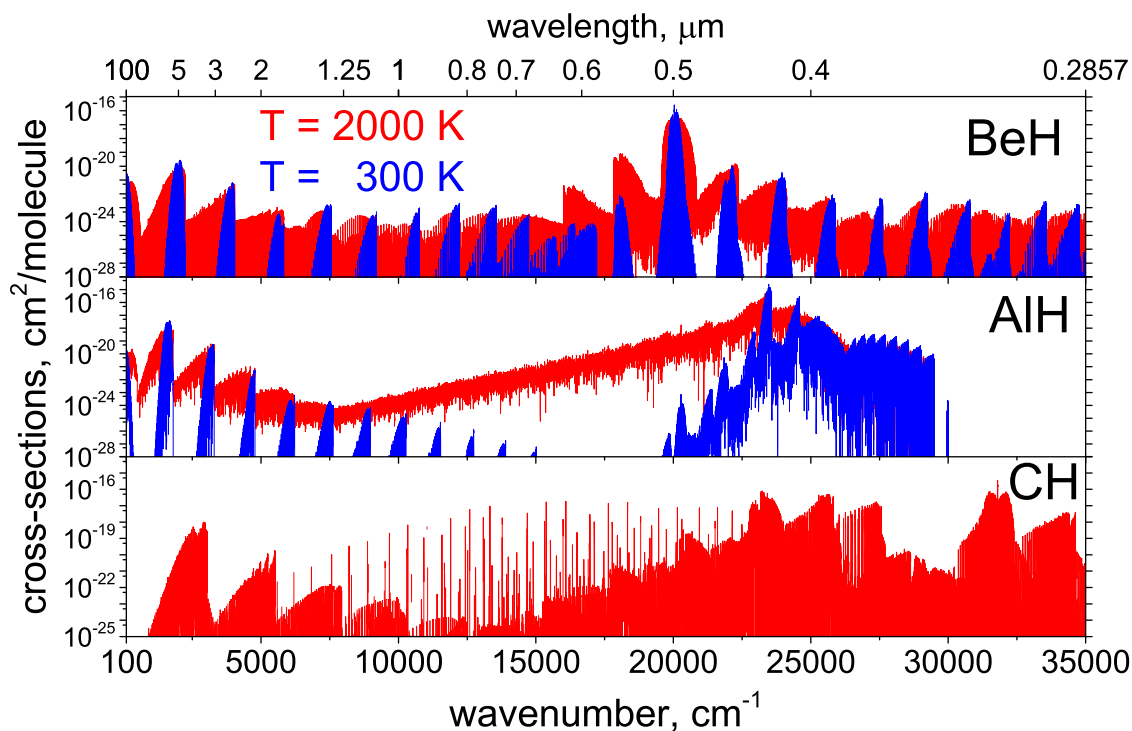


Figure 7. Cross sections for alkaline earth monohydrides and CH. BeH uses the updated ExoMol line list of Darby-Lewis et al. [138], AlH is the new ExoMol line list [76] and CH is the empirical work of Masseron et al. [83]; the CH line list is only defined for $T > 1000$ K.

Figure 8 shows temperature dependent cross sections for HCl, HS, CrH, and OH.

HCl: the line list used to generate the HCl cross sections given in Figure 8 was generated alongside line lists for other hydrogen halides, namely HF, HBr and HI, using semi-empirical methods by Li. et al. [86,143].

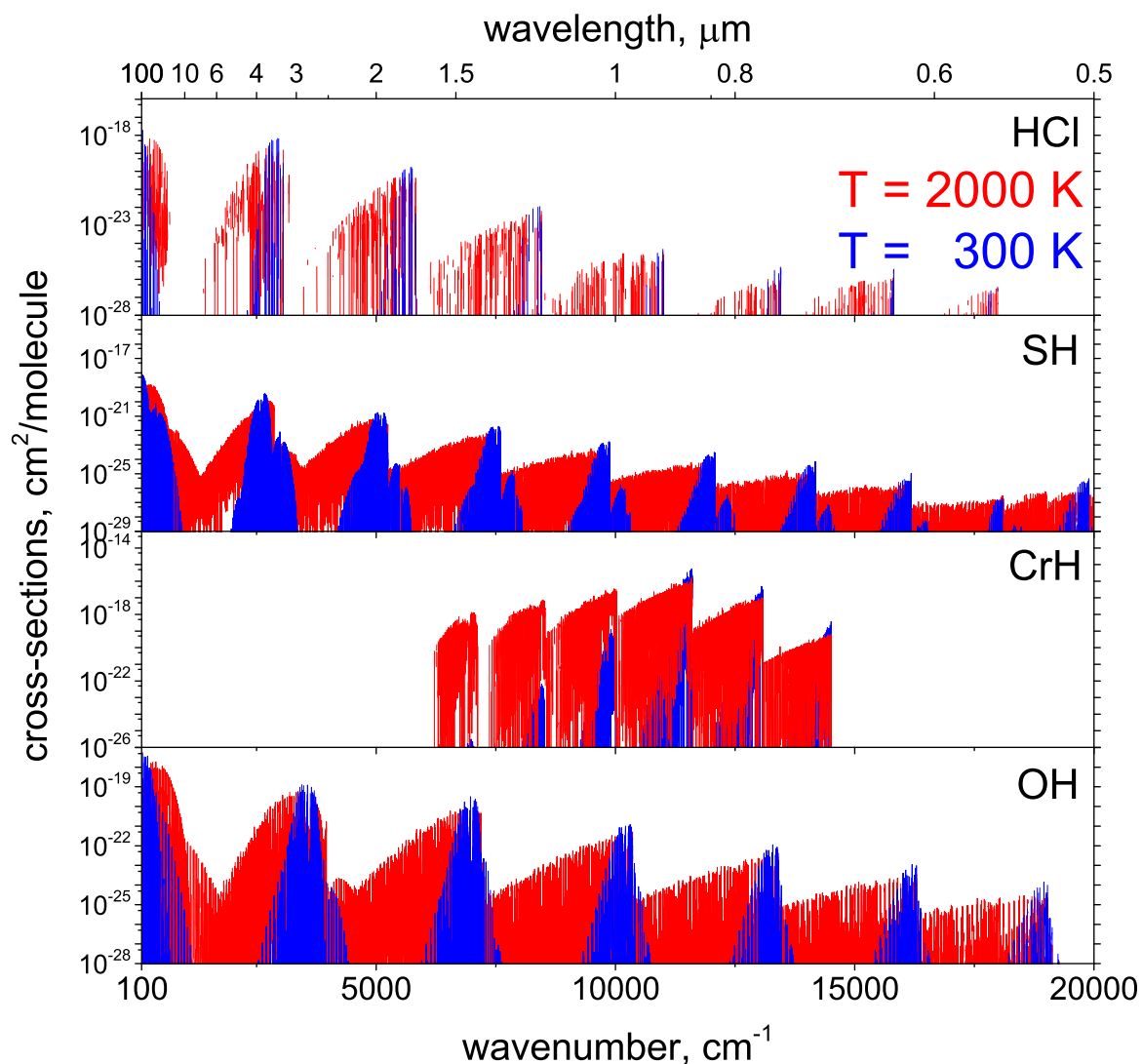


Figure 8. Cross sections for monohydrides: an empirical list due to Li. et al. [86] for HCl, an ExoMol line list for mercapto radical SH [74], chromium hydride [91]. The OH data are taken from HITEMP [4].

Figure 9 shows cross sections for NaCl, KCl, PO, PN and CS.

NaCl and **KCl**: cross sections are shown in Figure 9. These species have large transition dipoles and hence strong transitions, and they are thought to be of importance for studies of hot super-Earths [20].

PO: phosphorus monoxide has been detected in a number of locations in space: red Supergiant Star VY Canis Majoris [144], in the wind of the oxygen-rich AGB star IK Tauri [145], and in star-forming regions [146,147]. The ExoMol line list covers transitions within the $X^2\Pi$ ground electronic state.

PN: it is an important molecule used to probe different regions of the interstellar medium (ISM). The ExoMol line list for PN covers just pure rotation–vibration transitions.

CS: cross sections in Figure 9 illustrate the temperature dependence of the CS spectra as generated using the comprehensive vibration–rotation ExoMol line lists for eight isotopologues of carbon monosulphide (CS) ($^{12}\text{C}^{32}\text{S}$, $^{12}\text{C}^{33}\text{S}$, $^{12}\text{C}^{34}\text{S}$, $^{12}\text{C}^{36}\text{S}$, $^{13}\text{C}^{32}\text{S}$, $^{13}\text{C}^{33}\text{S}$, $^{13}\text{C}^{34}\text{S}$, $^{13}\text{C}^{36}\text{S}$) in their ground electronic states.

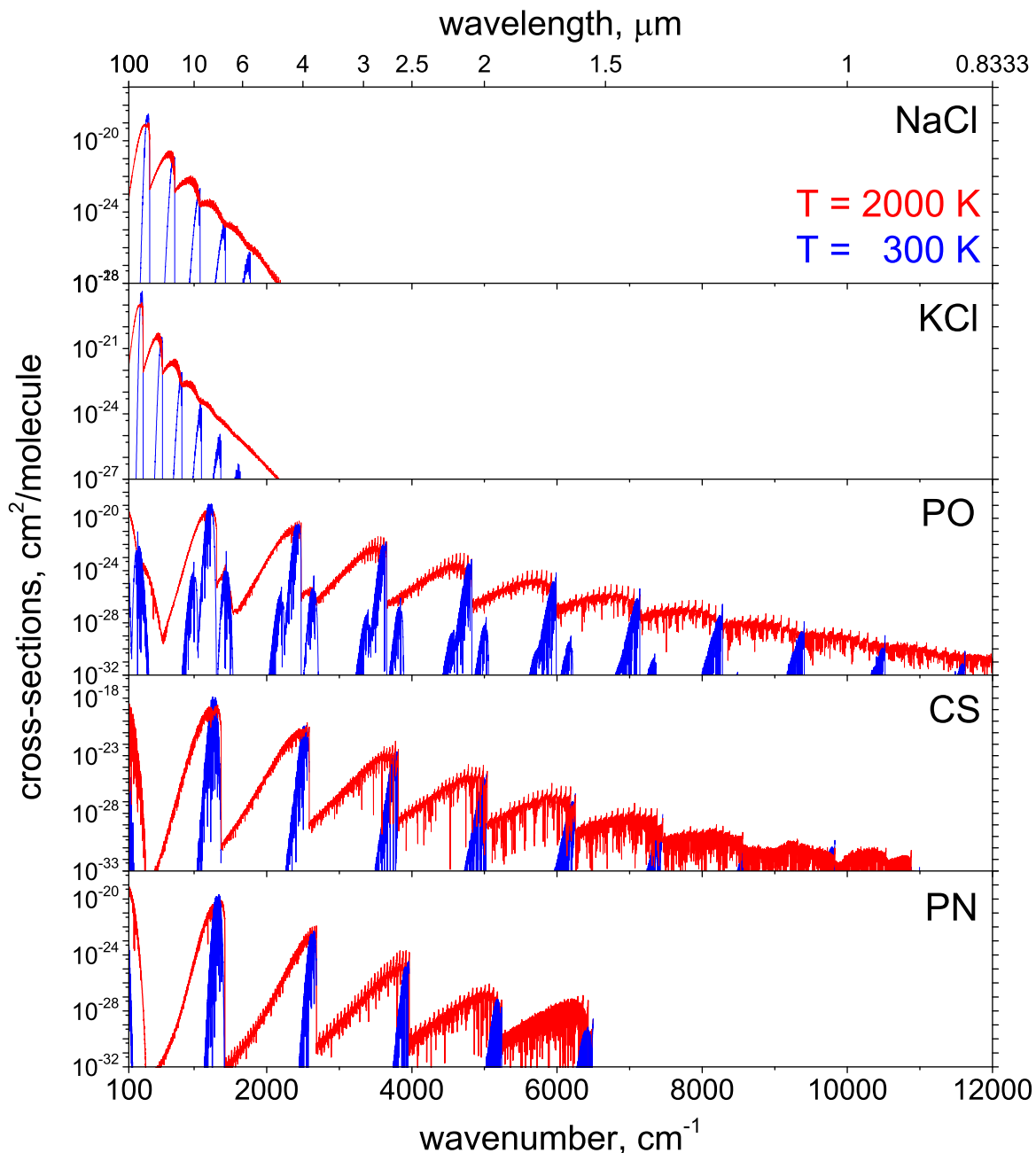


Figure 9. Cross sections generated from ExoMol line lists for sodium chloride [54], potassium chloride [54], phosphorous monoxide [71], carbon monosulfide [61] and phosphorous nitride [55].

Figure 10 shows cross sections for the important species CO plus CN, CP and CaO.

CO: cross sections for carbon monoxide are given in Figure 10. CO is ubiquitous throughout the spectra of cool stars [148] and brown dwarfs, and can clearly be seen in exoplanets [149,150]. CO is a very strongly bound species so the molecule survives at relatively high temperatures. As can be seen from the figure, its broadband spectrum changes from comprising a series of sharp bands to becoming quasi-continuous as the temperature is raised. Unlike the other species shown in this figure, the CO cross sections through the visible are simply given by rotation–vibration transitions. We note that Li et al. [8] improved their intensities by refining their CO ab initio dipole moment curve by fitting to experiment. This is not the usual practice [151], but Li et al. found that they could not get satisfactory results using a purely ab initio approach.

CN and CP: cross sections are shown in Figure 10. These two open shell or radical molecules have the same electronic structure and their spectra are dominated by the $A^2\Pi-X^2\Sigma^+$ and $B^2\Sigma^+-X^2\Sigma^+$ bands, which for CN lie in the red and violet regions of the visible. For the heavier CP radical, these bands are shifted to longer wavelengths.

CaO: cross sections for calcium oxide are given in Figure 10. CaO is unlikely to exist in the gas phase in dense atmospheres at 300 K, this spectrum is shown for the consistency. CaO has yet to be detected in space, but it is thought of as a possible component of super-Earth exoplanet atmospheres. CaO possesses transitions with notably large cross sections, which should facilitate its detection.

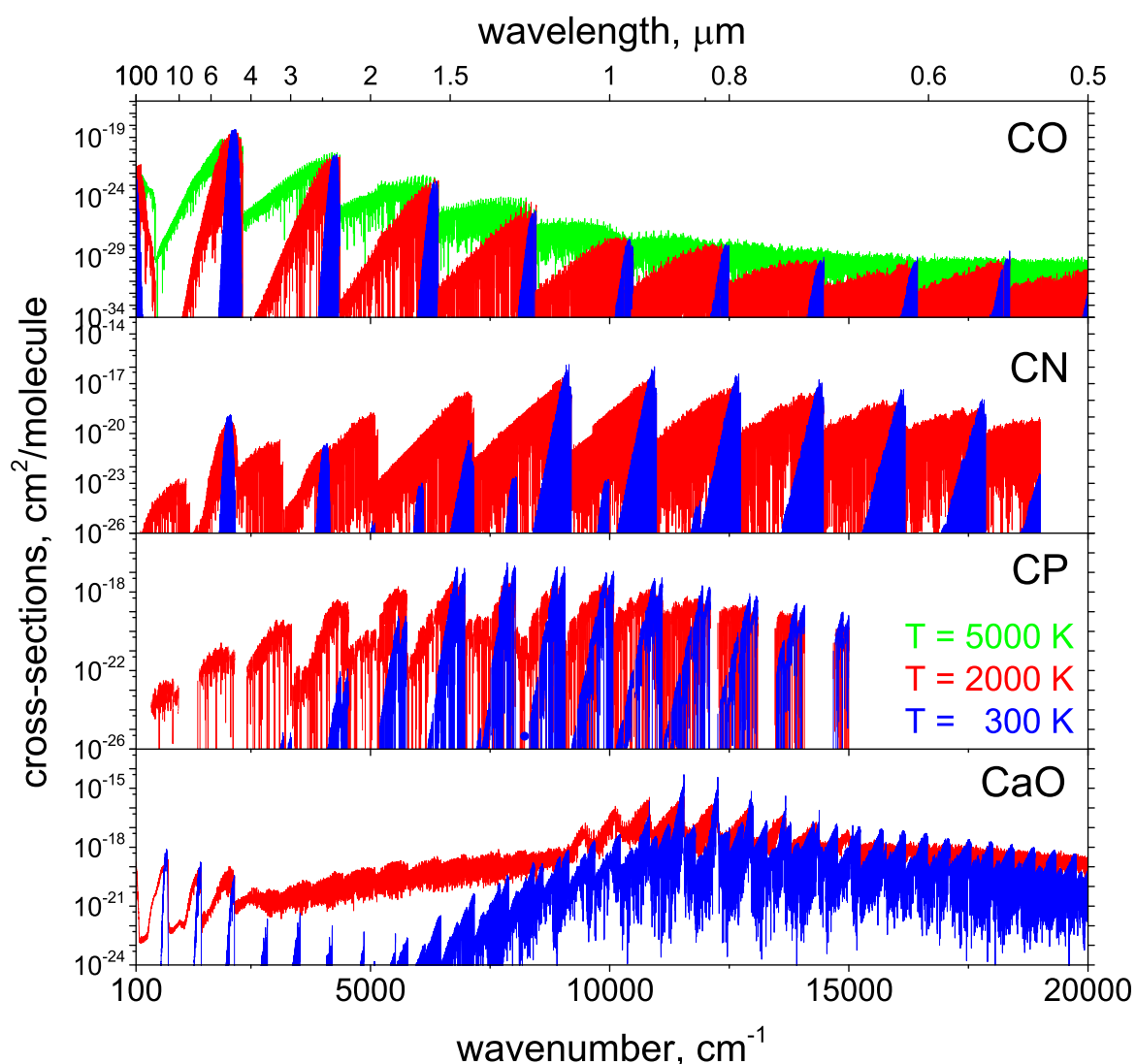


Figure 10. Cross sections for carbon monoxide, cyanide, carbon phosphide and calcium oxide. The CN [84] and CP [85] cross sections are based on empirical line lists from the Bernath group. The CaO data are taken from an ExoMol line list [62]. The CO [8] line list is based on an empirical dipole moment function.

Figure 11 shows cross sections for NO and PS.

NO and PS: are both radicals with $X^2\Pi$ electronic ground states. NO is an important species in the Earth's atmosphere and is likely to be so in oxygen-rich exoplanets. The current ExoMol line list [9] supersedes the one provided by HITEMP [4]. For NO, the transitions considered in the figure are all within the $X^2\Pi$ ground state manifold, while, for PS, the $B^2\Pi-X^2\Pi$ electronic band is also considered.

The equivalent electronic transition for NO, which is actually designated the A $^2\Pi - X^2\Pi$ band, lies well into the ultra violet at about 230 nm [152].

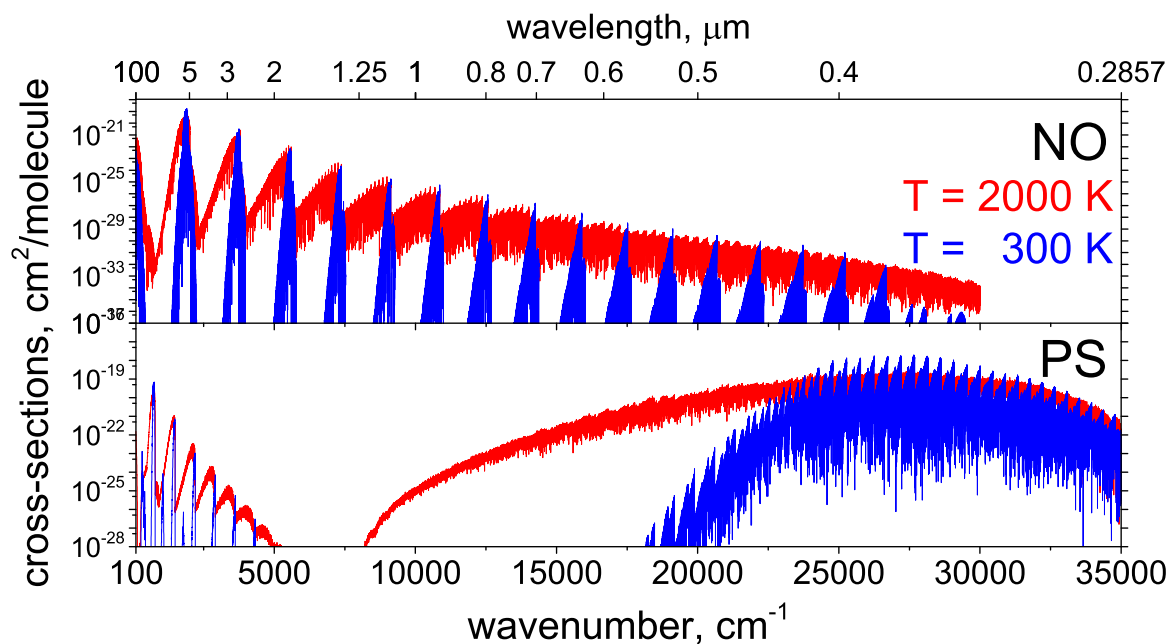


Figure 11. Cross sections generated from ExoMol line lists for nitric oxide [9] and phosphorous monosulfide [71].

Figure 12 shows cross sections for LiH, ScH, FeH and NH.

LiH cross sections are shown in Figure 12. They are based on ab initio calculations by Coppola et al. [80]. LiH is a four electron system so purely theoretical procedures should give reliable results. The spectrum of LiH is important for possible applications of the lithium test in brown dwarfs [153]. We note that very recently Bittner and Bernath [154] have constructed line lists for both LiF and LiCl.

ScH cross sections are shown in Figure 12. These were also based on an essentially ab initio line list, which contains an empirical adjustment for the band positions. Unlike LiH, ScH is a many-electron system with an open *d*-shell; such systems present considerable challenges from an ab initio perspective [155,156]; the provision of high accuracy line list for ScH will probably require further experimental input.

FeH cross sections, shown in Figure 12, are conversely based on experimental studies. FeH is an important stellar species, which has been observed in M and L dwarfs [87,157,158] as well as sunspots [159–161]. There is a strong need to use these laboratory studies to construct a rigorous theoretical model for the system, which can be used to generate line lists over an extended range of temperatures and wavelengths; however, ab initio calculations on the system remain a challenge [162].

NH: an empirical line list for NH from the Bernath group [82] covering rotation–vibrational transitions within the X $^3\Sigma^-$ ground electronic state.

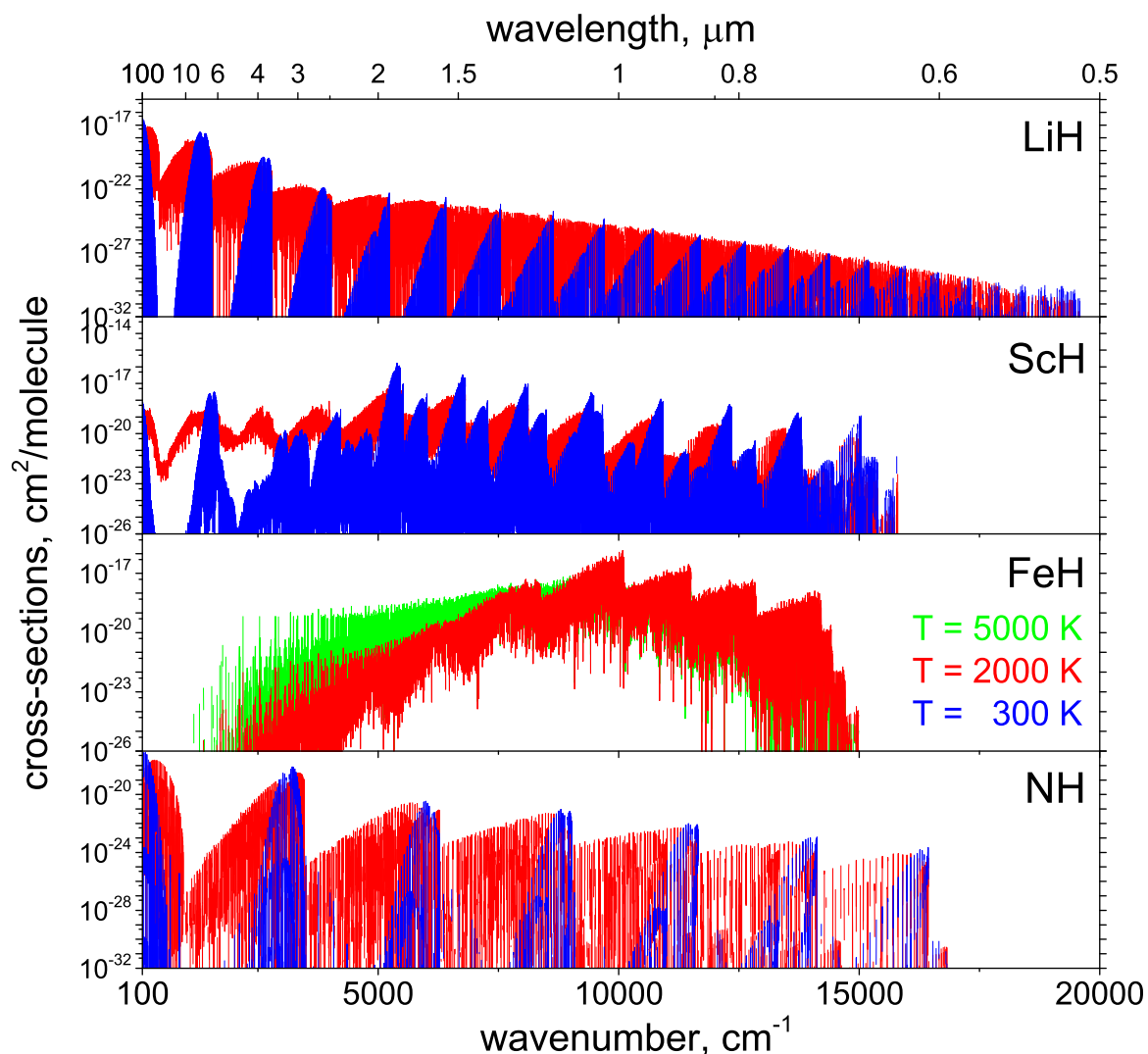


Figure 12. Cross sections for metal hydrides and NH. Line lists for lithium hydride [80] and scandium hydride [81] are theoretical while those for FeH and NH are derived from the experiments of the Bernath group [82,87,158,163].

Figure 13 shows cross sections for SiH, NaH and TiH.

SiH: is an accurate line list covering rotation–vibration transitions within the ground $X^2\Pi$ electronic state as well as transitions to the low-lying $A^2\Delta$ and a $4\Sigma^-$ states.

NaH cross sections are shown in Figure 13. NaH remains undetected in stellar spectra but is thought to be an important opacity source in M-dwarfs [164]. However, as our cross sections show the blue $A^2\Sigma^+ - X^2\Sigma^+$ band is extended and gives a rather flat band shape. This will make the clear detection of NaH in a stellar atmosphere difficult from its main electronic band.

TiH cross sections shown in Figure 13 represent an empirical line list for TiH from Burrows et al. [88].

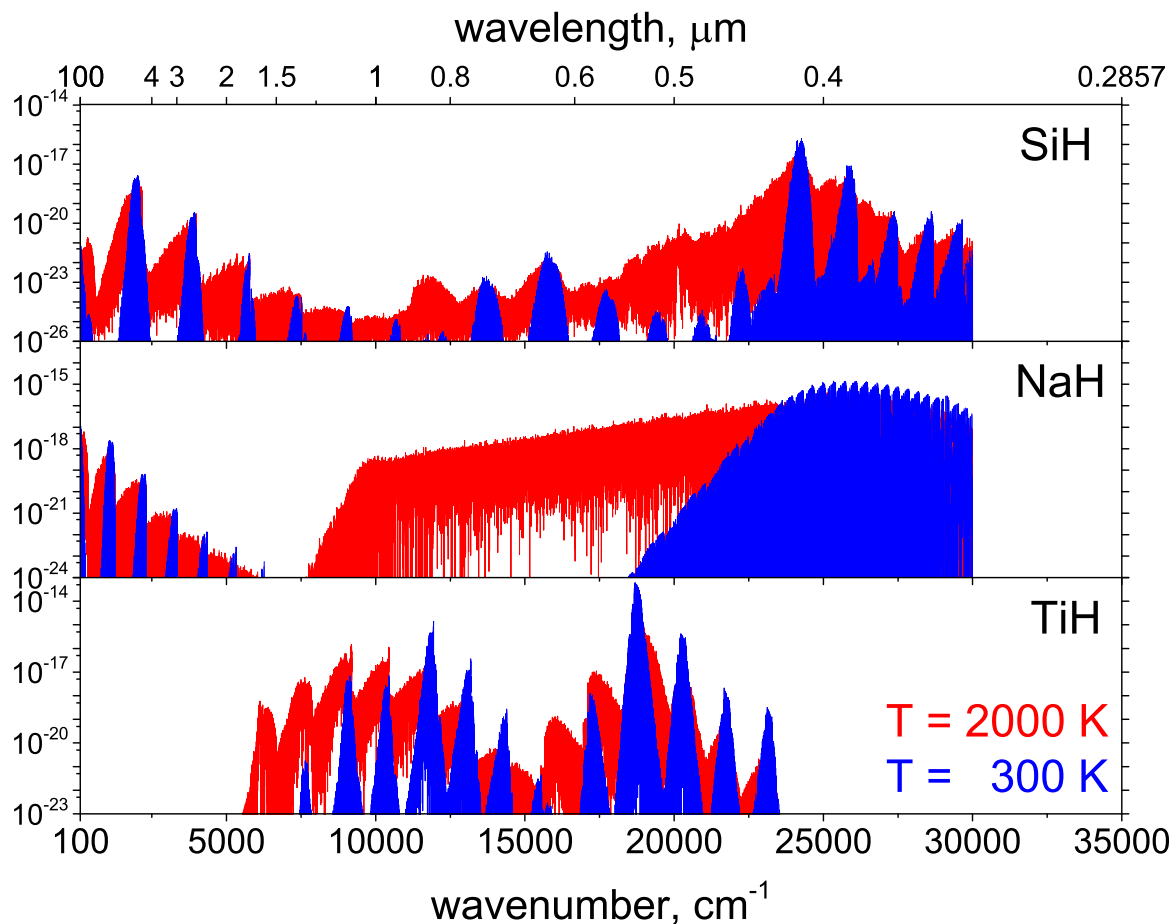


Figure 13. Cross sections for hydride species based on ExoMol line lists for sodium hydride [59] and silicon monohydride [72], and the empirical titanium monohydride line list of Burrows et al. [88].

Figure 13 shows cross sections for SiO, AlO, VO and TiO.

SiO cross sections are shown in Figure 14. SiO is a strongly bound molecule whose infrared spectrum is well-known in stars [165] and sunspots [166,167]. Its electronic spectrum has also been observed in sunspots [168]. At present, the ExoMol project has only provided a long-wavelength line list for SiO based on its temperature-dependent vibration–rotation and rotation spectrum. Work is in progress providing a companion line list covering its electronic bands starting from ab initio potential energy curves recently calculated by Bauschlicher Jr. et al. [169]. In order to illustrate the UV spectra of SiO, Figure 14 also shows cross sections from Kurucz’s database [170].

AlO: the spectrum of aluminium monoxide is illustrated in Figure 14. This spectrum is actually important for plasma diagnostics [171,172]. Rather remarkably, the only previous AlO line list [173], which was prepared for plasma studies, only provided relative as opposed to absolute line intensities.

VO cross sections are shown in Figure 14. The VO spectrum is heavily overlapped by that of TiO and the two molecules often occur together. VO spectral signatures are important for classifying late M dwarfs [174,175], and it is one of the dominant species in the spectra of young hot brown dwarfs [175–177]. VO is thought to be present in the atmosphere of hot Jupiter exoplanets [178].

TiO cross sections are shown in Figure 14. TiO is a well-known and important molecule in the atmosphere of M-dwarf stars [179]. Detections in the atmospheres of exoplanets are also beginning to be reported [180–182]. The figure is based on the line list of Schwenke et al. [89]; there is also a line list due to Plez [12], which has been updated in a recent release of the VALD database [183]. However, there are known problems with the available spectroscopic data on TiO (see Hoeijmakers et al. [26], for example). An ExoMol TiO line list is currently nearing completion [184]; this line list will make

use of the MARVEL study on TiO [43], which leads to more accurate transition frequencies than are provided by the currently available line lists.

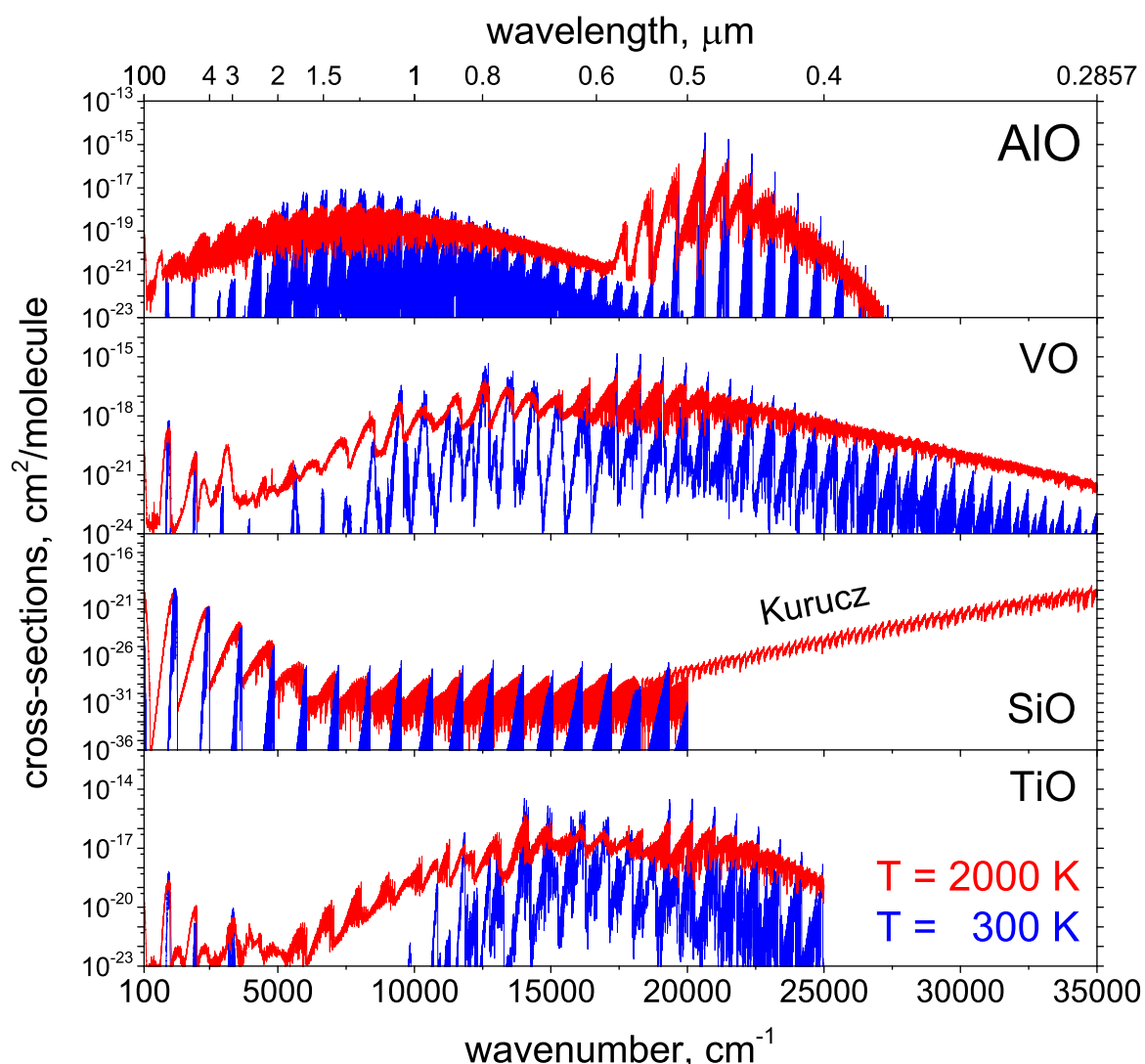


Figure 14. Cross sections for metal oxides generated using ExoMol line lists for silicon monoxide [52], aluminium monoxide [58] and vanadium monoxide [67]. The titanium monoxide cross sections are based on the computed line list due to Schwenke [89]. Also shown are short-wavelength silicon monoxide cross sections generated using line data from the database due to Kurucz [170].

Figure 15 gives cross sections for the open shell diatomic species C_2 and of the important molecular ion H_3^+ .

C_2 has a long spectroscopic history [185,186]. In astronomical objects, its spectrum has been observed via at least six distinct electronic bands, with other band systems required to explain observed populations. An empirical line list for the Swan system was provided by Brooke et al. [187]; the figure shows cross sections generated using the newly constructed ExoMol line list [77], which considers transitions between the eight lowest electronic states in the system. Given the many perturbations between the electronic states that are hard to model and that there are astronomically observed bands not covered by this eight-state model, further work on C_2 will undoubtedly be needed.

H_3^+ : the spectrum of H_3^+ given in Figure 15 is based on ab initio calculations, which have proved themselves to be very accurate for this molecular ion [188]. H_3^+ is an unusual species in that it has no (allowed [189]) rotational spectrum and no known electronic spectrum leaving only rotation–vibration

transitions. These are well-known in the ionospheres of solar system gas giant planets [190] but have yet to be observed in hot Jupiter exoplanets [191], where they might be thought to be prominent. However, the cooling provided by H_3^+ infrared emissions appears to be the key for the stability of atmospheres of giant extrasolar planets close to their host star [192]. This has made H_3^+ cooling functions of great importance [193,194]. Similarly H_3^+ has yet to be observed in stellar or brown dwarf spectra, but H_3^+ is the main source of electrons in objects such as cool white dwarfs [195]. The partition function of H_3^+ [196] thus controls the amount of H^- present, which, in turn, dominates the opacity. A line list for H_2D^+ [197] is also available.

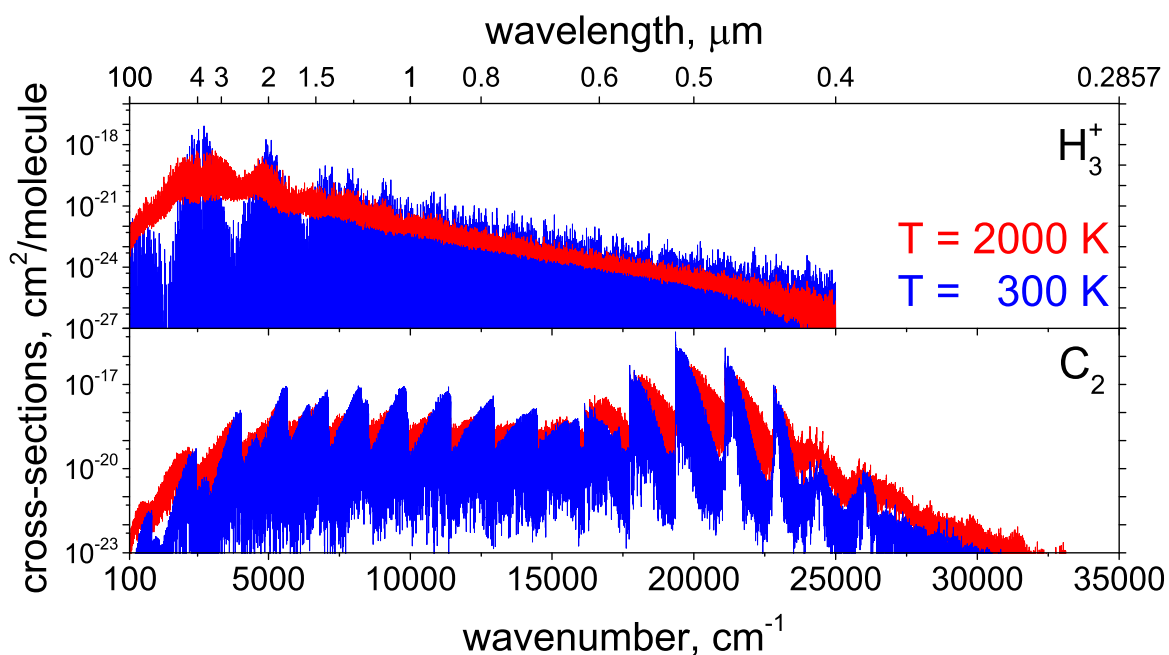


Figure 15. Cross sections based on ExoMol line lists for carbon dimer [77] and H_3^+ molecular ion [69].

4. Conclusions

Compiling molecular opacity functions requires a large range of spectroscopic data on a large range of molecules. As discussed in this article, for many key species, there are now extensive line lists available that can be used to compute temperature-dependent opacity functions. This is a process of constant improvement and immediate improvements are indeed identified for several species discussed above. Here, we consider what species may be missing from the current compilations.

In their validation of the well-used BT–Settl model [97] atmospheres for M-dwarfs, Rajpurohit et al. [164] identified only AlH, NaH and CaOH as key species for which data was missing. In response to this, the ExoMol project has provided spectroscopic line lists for AlH [76] and NaH [59]; this leaves CaOH, which has a strong band in the visible at 557 nm , as the one key missing species.

The chemistry of oxygen-rich M-dwarf stars is somewhat simpler than that of carbon-rich stars. There are a number of carbon-containing species for which reliable line lists are not available, notably acetylene (HCCH) and C_3 . Acetylene spectra are well-studied experimentally [44,198,199] and recently Lyulin and Perevalov [90] produced an effective-Hamiltonian based, empirical $^{12}\text{C}_2\text{H}_2$ line list. Work on an ExoMol acetylene line list is nearing completion. Jørgensen et al. [200] produced an early, purely ab initio line list for C_3 . They demonstrated the importance of this species for models of cool carbon stars, but their line list cannot be considered reliable by modern standards where ab initio methods have improved considerably and tuning models to experimental data is now routine. The construction of an improved C_3 line list is underway as part of the ExoMol project. Both ExoMol and TheoReTS are considering line lists for higher hydrocarbons that are needed for studies of exoplanets.

Transition metal containing diatomics provide strong sources of opacities since these open shell species often display strong electronic transitions in the near infrared and visible i.e., near the peak of the stellar flux for a cool star. A few of these species, notably TiO, VO, FeH, ScH and TiH, are considered above but there are many more possible candidates. These include CrH [201], MnH [202] and MgO [78] for which ExoMol has near complete line lists, and species such NiH, ZrO, YO, FeO. Carbides, nitrides and even sulfide species may also need to be considered in due course. Performing accurate ab initio electronic structure calculation on transition metal containing molecules remains very difficult [155,156].

Recent observations have identified a whole new class of exoplanets with masses somewhat larger than the Earth's and orbits close to their host stars. These hot rocky super-Earths, lava planets or magma planets as they are variously known as are just beginning to be characterized [116]. Even though at this point the molecular composition of their atmosphere is essentially unknown, study of these bodies will create demands for spectroscopic data and opacities for a whole range of new molecules. We recently reviewed the data needs for hot super-Earth exoplanets [20] and refer any interested reader to that article.

Finally, line broadening must be mentioned. Molecular transitions undergo broadening due to temperature and pressure effects. While temperature-induced Doppler broadening is straightforward to model, pressure broadening is more difficult because its importance is, at least in principle, different for every transition. Broadening parameters for key collision broadeners such as H₂ and He at elevated temperatures are largely missing. Approximate methods are being used to fill this void for key molecules such as water [182,203,204]. We have implemented a systematic and complete if approximate broadening "diet" [205] as part of the ExoMol data base [50]. This allows the generation of both temperature- and pressure-dependent cross sections using our program ExoCross [48]. However, there remains much work to be done in both improving temperature-dependent models for line broadening and providing the appropriate broadening parameters.

Author Contributions: Both authors contributed equally.

Acknowledgments: We thank the members of the ExoMol team for their work on this project. The ExoMol project was funded by the ERC Advanced Investigator Project 267219 and is currently supported by UK STFC under grant ST/M001334/1.

Conflicts of Interest: The authors declare no conflict of interest.

References

1. Sharp, C.M.; Burrows, A. Atomic and Molecular Opacities for Brown Dwarf and Giant Planet Atmospheres. *Astrophys. J. Suppl.* **2007**, *168*, 140.
2. Gordon, I.E.; Rothman, L.S.; Hill, C.; Kochanov, R.V.; Tan, Y.; Bernath, P.F.; Birk, M.; Boudon, V.; Campargue, A.; Chance, K.V.; et al. The HITRAN 2016 molecular spectroscopic database. *J. Quant. Spectrosc. Radiat. Transf.* **2017**, *203*, 3–69.
3. Schreier, F.; Staedt, S.; Hedelt, P.; Godolt, M. Transmission Spectroscopy with the ACE-FTS Infrared Spectral Atlas of Earth: A Model Validation and Feasibility Study. *Mol. Astrophys.* **2018**, *11*, 1–22.
4. Rothman, L.S.; Gordon, I.E.; Barber, R.J.; Dothe, H.; Gamache, R.R.; Goldman, A.; Perevalov, V.I.; Tashkun, S.A.; Tennyson, J. HITEMP, the High-Temperature Molecular Spectroscopic Database. *J. Quant. Spectrosc. Radiat. Transf.* **2010**, *111*, 2139–2150.
5. Polyansky, O.L.; Kyuberis, A.A.; Zobov, N.F.; Tennyson, J.; Yurchenko, S.N.; Lodi, L. ExoMol molecular line lists XXX: A complete high-accuracy line list for water. *Mon. Not. R. Astron. Soc.* **2018**, in press.
6. Tashkun, S.A.; Perevalov, V.I. CDSD-4000: High-resolution, high-temperature carbon dioxide spectroscopic databank. *J. Quant. Spectrosc. Radiat. Transf.* **2011**, *112*, 1403–1410.
7. Huang, X.; Schwenke, D.W.; Freedman, R.S.; Lee, T.J. Ames-2016 Line Lists for 13 Isotopologues of CO₂: Updates, Consistency, and Remaining Issues. *J. Quant. Spectrosc. Radiat. Transf.* **2017**, *203*, 224–241.

8. Li, G.; Gordon, I.E.; Rothman, L.S.; Tan, Y.; Hu, S.M.; Kass, S.; Campargue, A.; Medvedev, E.S. Rovibrational line lists for nine isotopologues of the CO molecule in the $X^1\Sigma^+$ ground electronic state. *Astrophys. J. Suppl.* **2015**, *216*, 15.
9. Wong, A.; Yurchenko, S.N.; Bernath, P.; Mueller, H.S.P.; McConkey, S.; Tennyson, J. ExoMol Line List XXI: Nitric Oxide (NO). *Mon. Not. R. Astron. Soc.* **2017**, *470*, 882–897.
10. Brooke, J.S.A.; Bernath, P.F.; Western, C.M.; Sneden, C.; Afşar, M.; Li, G.; Gordon, I.E. Line strengths of rovibrational and rotational transitions in the ground state of {OH}. *J. Quant. Spectrosc. Radiat. Transf.* **2016**, *138*, 142–157.
11. Jørgensen, U.G.; Larsson, M.; Iwamae, A.; Yu, B. Line intensities for CH and their application to stellar atmospheres. *Astron. Astrophys.* **1996**, *315*, 204.
12. Plez, B. A new TiO line list. *Astron. Astrophys.* **1998**, *337*, 495–500.
13. Weck, P.F.; Schweitzer, A.; Stancil, P.C.; Hauschildt, P.H.; Kirby, K. The molecular line opacity of MgH in cool stellar atmospheres. *Astrophys. J.* **2003**, *582*, 1059–1065.
14. Bernath, P.F. Molecular astronomy of cool stars and sub-stellar objects. *Int. Rev. Phys. Chem.* **2009**, *28*, 681–709.
15. Tennyson, J.; Yurchenko, S.N. ExoMol: Molecular line lists for exoplanet and other atmospheres. *Mon. Not. R. Astron. Soc.* **2012**, *425*, 21–33.
16. Rey, M.; Nikitin, A.V.; Babikov, Y.L.; Tyuterev, V.G. TheoReTS—An information system for theoretical spectra based on variational predictions from molecular potential energy and dipole moment surfaces. *J. Mol. Spectrosc.* **2016**, *327*, 138–158.
17. Tinetti, G.; Vidal-Madjar, A.; Liang, M.C.; Beaulieu, J.P.; Yung, Y.; Carey, S.; Barber, R.J.; Tennyson, J.; Ribas, I.; Allard, N.; et al. Water vapour in the atmosphere of a transiting extrasolar planet. *Nature* **2007**, *448*, 169–171.
18. Tinetti, G.; Encrenaz, T.; Coustenis, A. Spectroscopy of planetary atmospheres in our Galaxy. *Astron. Astrophys. Rev.* **2013**, *21*, 1–65.
19. Tennyson, J. Accurate variational calculations for line lists to model the vibration rotation spectra of hot astrophysical atmospheres. *WIREs Comput. Mol. Sci.* **2012**, *2*, 698–715.
20. Tennyson, J.; Yurchenko, S.N. Laboratory spectra of hot molecules: Data needs for hot super-Earth exoplanets. *Mol. Astrophys.* **2017**, *8*, 1–18.
21. Yurchenko, S.N.; Lodi, L.; Tennyson, J.; Stolyarov, A.V. Duo: A general program for calculating spectra of diatomic molecules. *Comput. Phys. Commun.* **2016**, *202*, 262–275.
22. Tennyson, J.; Kostin, M.A.; Barletta, P.; Harris, G.J.; Polyansky, O.L.; Ramanlal, J.; Zobov, N.F. DVR3D: A program suite for the calculation of rotation–vibration spectra of triatomic molecules. *Comput. Phys. Commun.* **2004**, *163*, 85–116.
23. Yurchenko, S.N.; Thiel, W.; Jensen, P. Theoretical ROVibrational Energies (TROVE): A robust numerical approach to the calculation of rovibrational energies for polyatomic molecules. *J. Mol. Spectrosc.* **2007**, *245*, 126–140.
24. Tennyson, J.; Yurchenko, S.N. The ExoMol project: Software for computing molecular line lists. *Int. J. Quantum Chem.* **2017**, *117*, 92–103.
25. Yurchenko, S.N.; Tennyson, J.; Bailey, J.; Hollis, M.D.J.; Tinetti, G. Spectrum of hot methane in astronomical objects using a comprehensive computed line list. *Proc. Natl. Acad. Sci. USA* **2014**, *111*, 9379–9383.
26. Hoeijmakers, H.J.; de Kok, R.J.; Snellen, I.A.G.; Brogi, M.; Birkby, J.L.; Schwarz, H. A search for TiO in the optical high-resolution transmission spectrum of HD 209458b: Hindrance due to inaccuracies in the line database. *Astron. Astrophys.* **2015**, *575*, A20.
27. Partridge, H.; Schwenke, D.W. The determination of an accurate isotope dependent potential energy surface for water from extensive ab initio calculations and experimental data. *J. Chem. Phys.* **1997**, *106*, 4618–4639.
28. Yurchenko, S.N.; Barber, R.J.; Tennyson, J.; Thiel, W.; Jensen, P. Towards efficient refinement of molecular potential energy surfaces: Ammonia as a case study. *J. Mol. Spectrosc.* **2011**, *268*, 123–129.
29. Tennyson, J.; Hill, C.; Yurchenko, S.N. Data structures for ExoMol: Molecular line lists for exoplanet and other atmospheres. *AIP Conf. Proc.* **2013**, *1545*, 186–195.
30. Barber, R.J.; Strange, J.K.; Hill, C.; Polyansky, O.L.; Mellau, G.C.; Yurchenko, S.N.; Tennyson, J. ExoMol line lists—III. An improved hot rotation–vibration line list for HCN and HNC. *Mon. Not. R. Astron. Soc.* **2014**, *437*, 1828–1835.

31. Furtenbacher, T.; Császár, A.G.; Tennyson, J. MARVEL: Measured active rotational-vibrational energy levels. *J. Mol. Spectrosc.* **2007**, *245*, 115–125.
32. Furtenbacher, T.; Császár, A.G. MARVEL: Measured active rotational-vibrational energy levels. II. Algorithmic improvements. *J. Quant. Spectrosc. Radiat. Transf.* **2012**, *113*, 929–935.
33. Császár, A.G.; Czakó, G.; Furtenbacher, T.; Mátyus, E. An active database approach to complete rotational–vibrational spectra of small molecules. *Annu. Rep. Comput. Chem.* **2007**, *3*, 155–176.
34. Tennyson, J.; Bernath, P.F.; Brown, L.R.; Campargue, A.; Császár, A.G.; Daumont, L.; Gamache, R.R.; Hodges, J.T.; Naumenko, O.V.; Polyansky, O.L.; et al. A Database of Water Transitions from Experiment and Theory (IUPAC Technical Report). *Pure Appl. Chem.* **2014**, *86*, 71–83.
35. Tennyson, J.; Bernath, P.F.; Brown, L.R.; Campargue, A.; Carleer, M.R.; Császár, A.G.; Gamache, R.R.; Hodges, J.T.; Jenouvrier, A.; Naumenko, O.V.; et al. IUPAC critical Evaluation of the Rotational-Vibrational Spectra of Water Vapor. Part I. Energy Levels and Transition Wavenumbers for H₂¹⁷O and H₂¹⁸O. *J. Quant. Spectrosc. Radiat. Transf.* **2009**, *110*, 573–596.
36. Tennyson, J.; Bernath, P.F.; Brown, L.R.; Campargue, A.; Carleer, M.R.; Császár, A.G.; Daumont, L.; Gamache, R.R.; Hodges, J.T.; Naumenko, O.V.; et al. IUPAC critical Evaluation of the Rotational-Vibrational Spectra of Water Vapor. Part II. Energy Levels and Transition Wavenumbers for HD¹⁶O, HD¹⁷O, and HD¹⁸O. *J. Quant. Spectrosc. Radiat. Transf.* **2010**, *111*, 2160–2184.
37. Tennyson, J.; Bernath, P.F.; Brown, L.R.; Campargue, A.; Carleer, M.R.; Császár, A.G.; Daumont, L.; Gamache, R.R.; Hodges, J.T.; Naumenko, O.V.; et al. IUPAC critical evaluation of the rotational-vibrational spectra of water vapor. Part III. Energy levels and transition wavenumbers for H₂¹⁶O. *J. Quant. Spectrosc. Radiat. Transf.* **2013**, *117*, 29–80.
38. Tennyson, J.; Bernath, P.F.; Brown, L.R.; Campargue, A.; Császár, A.G.; Daumont, L.; Gamache, R.R.; Hodges, J.T.; Naumenko, O.V.; Polyansky, O.L.; et al. IUPAC critical evaluation of the rotational-vibrational spectra of water vapor. Part IV. Energy levels and transition wavenumbers for D₂¹⁶O, D₂¹⁷O and D₂¹⁸O. *J. Quant. Spectrosc. Radiat. Transf.* **2014**, *142*, 93–108.
39. Furtenbacher, T.; Szidarovszky, T.; Mátyus, E.; Fábri, C.; Császár, A.G. Analysis of the Rotational–Vibrational States of the Molecular Ion H₃⁺. *J. Chem. Theory Comput.* **2013**, *9*, 5471–5478.
40. Furtenbacher, T.; Szidarovszky, T.; Fábri, C.; Császár, A.G. MARVEL analysis of the rotational–vibrational states of the molecular ions H₂D⁺ and D₂H⁺. *Phys. Chem. Chem. Phys.* **2013**, *15*, 10181–10193.
41. Al Derzi, A.R.; Furtenbacher, T.; Yurchenko, S.N.; Tennyson, J.; Császár, A.G. MARVEL analysis of the measured high-resolution spectra of ¹⁴NH₃. *J. Quant. Spectrosc. Radiat. Transf.* **2015**, *161*, 117–130.
42. Furtenbacher, T.; Szabó, I.; Császár, A.G.; Bernath, P.F.; Yurchenko, S.N.; Tennyson, J. Experimental Energy Levels and Partition Function of the ¹²C₂ Molecule. *Astrophys. J. Suppl.* **2016**, *224*, 44.
43. McKemmish, L.K.; Masseron, T.; Sheppard, S.; Sandeman, E.; Schofield, Z.; Furtenbacher, T.; Császár, A.G.; Tennyson, J.; Sousa-Silva, C. MARVEL analysis of the measured high-resolution spectra of ⁴⁸Ti¹⁶O. *Astrophys. J. Suppl.* **2017**, *228*, 15.
44. Chubb, K.L.; Joseph, M.; Franklin, J.; Choudhury, N.; Furtenbacher, T.; Császár, A.G.; Gaspard, G.; Oguoko, P.; Kelly, A.; Yurchenko, S.N.; et al. MARVEL analysis of the measured high-resolution spectra of C₂H₂. *J. Quant. Spectrosc. Radiat. Transf.* **2018**, *204*, 42–55.
45. Tóbiás, R.; Furtenbacher, T.; Császár, A.G.; Naumenko, O.V.; Tennyson, J.; Flaud, J.M.; Kumard, P.; Poirier, B. Critical Evaluation of Measured Rotational-Vibrational Transitions of Four Sulphur Isotopologues of S¹⁶O₂. *J. Quant. Spectrosc. Radiat. Transf.* **2018**, *208*, 152–163.
46. Chubb, K.L.; Naumenko, O.V.; Keely, S.; Bartolotto, S.; MacDonald, S.; Mukhtar, M.; Grachov, A.; White, J.; Coleman, E.; Hu, S.M.; et al. MARVEL analysis of the measured high-resolution rovibrational spectra of H₂S. *J. Quant. Spectrosc. Radiat. Transf.* **2018**, submitted.
47. McKemmish, L.K.; Goodhew, K.; Sheppard, S.; Bennet, A.; Martin, A.; Singh, A.; Sturgeon, C.; Godden, R.; Furtenbacher, T.; Császár, A.G.; et al. MARVEL analysis of the measured high-resolution spectra of ⁹⁰Zr¹⁶O. *Astrophys. J. Suppl.* **2018**, to be submitted.
48. Yurchenko, S.N.; Al-Refai, A.F.; Tennyson, J. ExoCross: A general program for generating spectra from molecular line lists. *Astron. Astrophys.* **2018**, doi:10.1051/0004-6361/201732531.
49. Hill, C.; Yurchenko, S.N.; Tennyson, J. Temperature-dependent molecular absorption cross sections for exoplanets and other atmospheres. *Icarus* **2013**, *226*, 1673–1677.

50. Tennyson, J.; Yurchenko, S.N.; Al-Refaie, A.F.; Barton, E.J.; Chubb, K.L.; Coles, P.A.; Diamantopoulou, S.; Gorman, M.N.; Hill, C.; Lam, A.Z.; et al. The ExoMol database: Molecular line lists for exoplanet and other hot atmospheres. *J. Mol. Spectrosc.* **2016**, *327*, 73–94.
51. Yadin, B.; Vaness, T.; Conti, P.; Hill, C.; Yurchenko, S.N.; Tennyson, J. ExoMol Molecular line lists: I The rovibrational spectrum of BeH, MgH and CaH the $X^2\Sigma^+$ state. *Mon. Not. R. Astron. Soc.* **2012**, *425*, 34–43.
52. Barton, E.J.; Yurchenko, S.N.; Tennyson, J. ExoMol Molecular line lists—II. The ro-vibrational spectrum of SiO. *Mon. Not. R. Astron. Soc.* **2013**, *434*, 1469–1475.
53. Yurchenko, S.N.; Tennyson, J. ExoMol line lists IV: The rotation–vibration spectrum of methane up to 1500 K. *Mon. Not. R. Astron. Soc.* **2014**, *440*, 1649–1661.
54. Barton, E.J.; Chiu, C.; Golpayegani, S.; Yurchenko, S.N.; Tennyson, J.; Frohman, D.J.; Bernath, P.F. ExoMol Molecular line lists—V. The ro-vibrational spectra of NaCl and KCl. *Mon. Not. R. Astron. Soc.* **2014**, *442*, 1821–1829.
55. Yorke, L.; Yurchenko, S.N.; Lodi, L.; Tennyson, J. ExoMol line lists VI: A high temperature line list for Phosphorus Nitride. *Mon. Not. R. Astron. Soc.* **2014**, *445*, 1383–1391.
56. Sousa-Silva, C.; Al-Refaie, A.F.; Tennyson, J.; Yurchenko, S.N. ExoMol line lists—VII. The rotation–vibration spectrum of phosphine up to 1500 K. *Mon. Not. R. Astron. Soc.* **2015**, *446*, 2337–2347.
57. Al-Refaie, A.F.; Yurchenko, S.N.; Yachmenev, A.; Tennyson, J. ExoMol line lists—VIII: A variationally computed line list for hot formaldehyde. *Mon. Not. R. Astron. Soc.* **2015**, *448*, 1704–1714.
58. Patrascu, A.T.; Tennyson, J.; Yurchenko, S.N. ExoMol molecular line lists: VII: The spectrum of AlO. *Mon. Not. R. Astron. Soc.* **2015**, *449*, 3613–3619.
59. Rivlin, T.; Lodi, L.; Yurchenko, S.N.; Tennyson, J.; Le Roy, R.J. ExoMol line lists X: The spectrum of sodium hydride. *Mon. Not. R. Astron. Soc.* **2015**, *451*, 5153–5157.
60. Pavlyuchko, A.I.; Yurchenko, S.N.; Tennyson, J. ExoMol line lists XI: A Hot Line List for nitric acid. *Mon. Not. R. Astron. Soc.* **2015**, *452*, 1702–1706.
61. Paulose, G.; Barton, E.J.; Yurchenko, S.N.; Tennyson, J. ExoMol Molecular line lists—XII. Line lists for eight isotopologues of CS. *Mon. Not. R. Astron. Soc.* **2015**, *454*, 1931–1939.
62. Yurchenko, S.N.; Blissett, A.; Asari, U.; Vasilios, M.; Hill, C.; Tennyson, J. ExoMol Molecular line lists—XIII. The spectrum of CaO. *Mon. Not. R. Astron. Soc.* **2016**, *456*, 4524–4532.
63. Underwood, D.S.; Tennyson, J.; Yurchenko, S.N.; Huang, X.; Schwenke, D.W.; Lee, T.J.; Clausen, S.; Fateev, A. ExoMol line lists XIV: A line list for hot SO₂. *Mon. Not. R. Astron. Soc.* **2016**, *459*, 3890–3899.
64. Al-Refaie, A.F.; Polyansky, O.L.; Ovsyannikov, I.R.; Tennyson, J.; Yurchenko, S.N. ExoMol line lists XV: A hot line-list for hydrogen peroxide. *Mon. Not. R. Astron. Soc.* **2016**, *461*, 1012–1022.
65. Azzam, A.A.A.; Yurchenko, S.N.; Tennyson, J.; Naumenko, O.V. ExoMol line lists XVI: A Hot Line List for H₂S. *Mon. Not. R. Astron. Soc.* **2016**, *460*, 4063–4074.
66. Underwood, D.S.; Tennyson, J.; Yurchenko, S.N.; Clausen, S.; Fateev, A. ExoMol line lists XVII: A line list for hot SO₃. *Mon. Not. R. Astron. Soc.* **2016**, *462*, 4300–4313.
67. McKemmish, L.K.; Yurchenko, S.N.; Tennyson, J. ExoMol Molecular line lists—XVIII. The spectrum of Vanadium Oxide. *Mon. Not. R. Astron. Soc.* **2016**, *463*, 771–793.
68. Polyansky, O.L.; Kyuberis, A.A.; Lodi, L.; Tennyson, J.; Ovsyannikov, R.I.; Zobov, N. ExoMol molecular line lists XIX: High accuracy computed line lists for H₂¹⁷O and H₂¹⁸O. *Mon. Not. R. Astron. Soc.* **2017**, *466*, 1363–1371.
69. Mizus, I.I.; Alijah, A.; Zobov, N.F.; Kyuberis, A.A.; Yurchenko, S.N.; Tennyson, J.; Polyansky, O.L. ExoMol molecular line lists XX: A comprehensive line list for H₃⁺. *Mon. Not. R. Astron. Soc.* **2017**, *468*, 1717–1725.
70. Owens, A.; Yurchenko, S.N.; Yachmenev, A.; Thiel, W.; Tennyson, J. ExoMol molecular line lists XXII. The rotation–vibration spectrum of silane up to 1200 K. *Mon. Not. R. Astron. Soc.* **2017**, *471*, 5025–5032.
71. Prajapat, L.; Jagoda, P.; Lodi, L.; Gorman, M.N.; Yurchenko, S.N.; Tennyson, J. ExoMol molecular line lists XXIII. Spectra of PO and PS. *Mon. Not. R. Astron. Soc.* **2017**, *472*, 3648–3658.
72. Yurchenko, S.N.; Sinden, F.; Lodi, L.; Hill, C.; Gorman, M.N.; Tennyson, J. ExoMol Molecular line lists—XXIV: A new hot line list for silicon monohydride, SiH. *Mon. Not. R. Astron. Soc.* **2018**, *473*, 5324–5333.
73. Upadhyay, A.; Conway, E.K.; Tennyson, J.; Yurchenko, S.N. ExoMol Molecular line lists—XXV: A hot line list for silicon sulphide, SiS. *Mon. Not. R. Astron. Soc.* **2018**, doi:10.1093/mnras/sty998.
74. Yurchenko, S.N.; Bond, W.; Gorman, M.N.; Lodi, L.; McKemmish, L.K.; Nunn, W.; Shah, R.; Tennyson, J. ExoMol Molecular line lists—XXVI: Spectra of SH and NS. *Mon. Not. R. Astron. Soc.* **2018**, doi:10.1093/mnras/sty939.

75. Mant, B.P.; Yachmenev, A.; Tennyson, J.; Yurchenko, S.N. ExoMol molecular line lists—XXVII: Spectra of C_2H_4 . *Mon. Not. R. Astron. Soc.* **2018**, in press.
76. Yurchenko, S.N.; Williams, H.; Leyland, P.C.; Lodi, L.; Tennyson, J. ExoMol line lists XXVIII: The rovibronic spectrum of AlH. *Mon. Not. R. Astron. Soc.* **2018**, in press.
77. Yurchenko, S.N.; Szabo, I.; Pyatenko, E.; Tennyson, J. ExoMol Molecular line lists XXXI: The spectrum of C_2 . *Mon. Not. R. Astron. Soc.* **2018**, in press.
78. Li, H.Y.; Patrascu, A.; Tennyson, J.; Yurchenko, S.N. ExoMol molecular line lists XXXII: The rovibronic spectrum of MgO. *Mon. Not. R. Astron. Soc.* **2018**, to be submitted.
79. Yurchenko, S.N.; Barber, R.J.; Tennyson, J. A variationally computed hot line list for NH_3 . *Mon. Not. R. Astron. Soc.* **2011**, *413*, 1828–1834.
80. Coppola, C.M.; Lodi, L.; Tennyson, J. Radiative cooling functions for primordial molecules. *Mon. Not. R. Astron. Soc.* **2011**, *415*, 487–493.
81. Lodi, L.; Yurchenko, S.N.; Tennyson, J. The calculated rovibronic spectrum of scandium hydride, ScH. *Mol. Phys.* **2015**, *113*, 1559–1575.
82. Brooke, J.S.A.; Bernath, P.F.; Western, C.M.; van Hemert, M.C.; Groenenboom, G.C. Line strengths of rovibrational and rotational transitions within the $X^3\Sigma^-$ ground state of NH. *J. Chem. Phys.* **2014**, *141*, 054310.
83. Masseron, T.; Plez, B.; Van Eck, S.; Colin, R.; Daoutidis, I.; Godefroid, M.; Coheur, P.F.; Bernath, P.; Jorissen, A.; Christlieb, N. CH in stellar atmospheres: An extensive linelist. *Astron. Astrophys.* **2014**, *571*, A47.
84. Brooke, J.S.A.; Ram, R.S.; Western, C.M.; Li, G.; Schwenke, D.W.; Bernath, P.F. Einstein A Coefficients and Oscillator Strengths for the $A^2\Pi-X^2\Sigma^+$ (Red) and $B^2\Sigma^+-X^2\Sigma^+$ (Violet) Systems and Rovibrational Transitions in the $X^2\Sigma^+$ State of CN. *Astrophys. J. Suppl.* **2014**, *210*, 23.
85. Ram, R.S.; Brooke, J.S.A.; Western, C.M.; Bernath, P.F. Einstein A-values and oscillator strengths of the $A^2\Pi-X^2\Sigma^+$ system of CP. *J. Quant. Spectrosc. Radiat. Transf.* **2014**, *138*, 107–115.
86. Li, G.; Gordon, I.E.; Hajigeorgiou, P.G.; Coxon, J.A.; Rothman, L.S. Reference spectroscopic data for hydrogen halides, Part II: The line lists. *J. Quant. Spectrosc. Radiat. Transf.* **2013**, *130*, 284–295.
87. Wende, S.; Reiners, A.; Seifahrt, A.; Bernath, P.F. CRIREs spectroscopy and empirical line-by-line identification of FeH molecular absorption in an M dwarf. *Astron. Astrophys.* **2010**, *523*, A58.
88. Burrows, A.; Dulick, M.; Bauschlicher, C.W.; Bernath, P.F.; Ram, R.S.; Sharp, C.M.; Milsom, J.A. Spectroscopic constants, abundances, and opacities of the TiH molecule. *Astrophys. J.* **2005**, *624*, 988–1002.
89. Schwenke, D.W. Opacity of TiO from a coupled electronic state calculation parametrized by ab initio and experimental data. *Faraday Discuss.* **1998**, *109*, 321–334.
90. Lyulin, O.M.; Perevalov, V.I. ASD-1000: High-resolution, high-temperature acetylene spectroscopic databank. *J. Quant. Spectrosc. Radiat. Transf.* **2017**, *201*, 94–103.
91. Burrows, A.; Ram, R.S.; Bernath, P.; Sharp, C.M.; Milsom, J.A. New CrH opacities for the study of L and brown dwarf atmospheres. *Astrophys. J.* **2002**, *577*, 986–992.
92. Owens, A.; Yachmenev, A.; Küpper, J.; Yurchenko, S.N.; Thiele, W. The rotation–vibration spectrum of methyl fluoride from first principles. *Phys. Chem. Chem. Phys.* **2018**, in press.
93. Voronin, B.A.; Tennyson, J.; Tolchenov, R.N.; Lugovskoy, A.A.; Yurchenko, S.N. A high accuracy computed line list for the HDO molecule. *Mon. Not. R. Astron. Soc.* **2010**, *402*, 492–496.
94. Allard, F.; Hauschildt, P.H.; Miller, S.; Tennyson, J. The influence of H_2O line blanketing on the spectra of cool dwarf stars. *Astrophys. J.* **1994**, *426*, L39–L41.
95. Tinetti, G.; Tennyson, J.; Griffiths, C.A.; Waldmann, I. Water in Exoplanets. *Philos. Trans. R. Soc. Lond. A* **2012**, *370*, 2749–2764.
96. Barber, R.J.; Tennyson, J.; Harris, G.J.; Tolchenov, R.N. A high accuracy computed water line list. *Mon. Not. R. Astron. Soc.* **2006**, *368*, 1087–1094.
97. Allard, F. The BT-Settl Model Atmospheres for Stars, Brown Dwarfs and Planets. In *IAU Symposium*; Booth, M., Matthews, B.C., Graham, J.R., Eds.; International Astronomical Union: Paris, France, 2014; Volume 299, pp. 271–272.
98. Rutkowski, L.; Foltynowicz, A.; Johansson, A.C.; Khodabakhsh, A.; Schmidt, F.M.; Kyuberis, A.A.; Zobov, N.F.; Polyansky, O.L.; Yurchenko, S.N.; Tennyson, J. An experimental water line list at 1950 K in the 6250–6670 cm^{-1} region. *J. Quant. Spectrosc. Radiat. Transf.* **2018**, *205*, 213–219.

99. Campargue, A.; Mikhailenko, S.N.; Vasilchenko, S.; Reynaud, C.; Beguier, S.; Cermak, P.; Mondelain, D.; Kassi, S.; Romanini, D. The absorption spectrum of water vapor in the 2.2 μm transparency window: High sensitivity measurements and spectroscopic database. *J. Quant. Spectrosc. Radiat. Transf.* **2017**, *189*, 407–416.
100. Rey, M.; Nikitin, A.V.; Tyuterev, V.G. Theoretical hot methane line list up T=2000 K for astrophysical applications. *Astrophys. J.* **2014**, *789*, 2.
101. Rey, M.; Nikitin, A.V.; Tyuterev, V.G. Accurate Theoretical Methane Line Lists in the Infrared up to 3000 K and Quasi-continuum Absorption/Emission Modeling for Astrophysical Applications. *Astrophys. J.* **2017**, *847*, 105.
102. Hargreaves, R.J.; Beale, C.A.; Michaux, L.; Irfan, M.; Bernath, P.F. Hot methane line lists for exoplanet and brown dwarf atmospheres. *Astrophys. J.* **2012**, *757*, 46.
103. Hargreaves, R.J.; Bernath, P.F.; Bailey, J.; Dulick, M. Empirical Line Lists and Absorption Cross Sections for Methane at High Temperatures. *Astrophys. J.* **2015**, *813*, 12.
104. Canty, J.I.; Lucas, P.W.; Tennyson, J.; Yurchenko, S.N.; Leggett, S.K.; Tinney, C.G.; Jones, H.R.A.; Burningham, B.; Pinfield, D.J.; Smart, R.L. Methane and Ammonia in the near-infrared spectra of late T dwarfs. *Mon. Not. R. Astron. Soc.* **2015**, *450*, 454–480.
105. Yurchenko, S.N.; Amundsen, D.S.; Tennyson, J.; Waldmann, I.P. A hybrid line list for CH₄ and hot methane continuum. *Astron. Astrophys.* **2017**, *605*, A95.
106. Fletcher, L.N.; Orton, G.S.; Teanby, N.A.; Irwin, P.G.J. Phosphine on Jupiter and Saturn from Cassini/CIRS. *Icarus* **2009**, *202*, 543–564.
107. Yurchenko, S.N. A theoretical room-temperature line list for ¹⁵NH₃. *J. Quant. Spectrosc. Radiat. Transf.* **2015**, *152*, 28–36.
108. Rey, M.; Delahaye, T.; Nikitin, A.V.; Tyuterev, V.G. First theoretical global line lists of ethylene (12 C₂H₄) spectra for the temperature range 50,700 K in the far-infrared for quantification of absorption and emission in planetary atmospheres. *Astron. Astrophys.* **2016**, *594*, A47.
109. Al-Refaie, A.F.; Ovsyannikov, R.I.; Polyansky, O.L.; Yurchenko, S.N.; Tennyson, J. A variationally calculated room temperature line-list for H₂O₂. *J. Mol. Spectrosc.* **2015**, *318*, 84–90.
110. Harris, G.J.; Polyansky, O.L.; Tennyson, J. Opacity data for HCN and HNC from a new ab initio linelist. *Astrophys. J.* **2002**, *578*, 657–663.
111. Harris, G.J.; Tennyson, J.; Kaminsky, B.M.; Pavlenko, Y.V.; Jones, H.R.A. Improved HCN/HNC linelist, model atmospheres synthetic spectra for WZ Cas. *Mon. Not. R. Astron. Soc.* **2006**, *367*, 400–406.
112. Mellau, G.C. Highly excited rovibrational states of HNC. *J. Mol. Spectrosc.* **2011**, *269*, 77–85.
113. Mellau, G.C. Complete experimental rovibrational eigenenergies of HCN up to 6880 cm⁻¹ above the ground state. *J. Chem. Phys.* **2011**, *134*, 234303.
114. Mellau, G.C. Rovibrational eigenenergy structure of the [H,C,N] molecular system. *J. Chem. Phys.* **2011**, *134*, 194302.
115. Harris, G.J.; Larner, F.C.; Tennyson, J.; Kaminsky, B.M.; Pavlenko, Y.V.; Jones, H.R.A. A H¹³CN/HN¹³C linelist, model atmospheres and synthetic spectra for carbon stars. *Mon. Not. R. Astron. Soc.* **2008**, *390*, 143–148.
116. Tsiaras, A.; Rocchetto, M.; Waldmann, I.P.; Tinetti, G.; Varley, R.; Morello, G.; Barton, E.J.; Yurchenko, S.N.; Tennyson, J. Detection of an atmosphere around the super-Earth 55 Cancri e. *Astrophys. J.* **2016**, *820*, 99.
117. Eriksson, K.; Gustafsson, B.; Jørgensen, U.G.; Nordlund, A. Effects of HCN molecules in carbon star atmospheres. *Astron. Astrophys.* **1984**, *132*, 37–44.
118. Barber, R.J.; Harris, G.J.; Tennyson, J. Temperature dependent partition functions and equilibrium constant for HCN and HNC. *J. Chem. Phys.* **2002**, *117*, 11239–11243.
119. Kaltenegger, L.; Henning, W.G.; Sasselov, D.D. Detecting volcanism on extrasolar planets. *Astron. J.* **2010**, *140*, 1370.
120. Hu, R.; Seager, S.; Bains, W. Photochemistry in terrestrial exoplanet atmospheres. II. H₂S and SO₂ photochemistry in anoxic atmospheres. *Astrophys. J.* **2013**, *769*, 6.
121. Whitehill, A.R.; Xie, C.; Hu, X.; Xie, D.; Guo, H.; Ono, S. Vibronic origin of sulfur mass-independent isotope effect in photoexcitation of SO₂ and the implications to the early earth's atmosphere. *Proc. Natl. Acad. Sci. USA* **2013**, *110*, 17697–17702.
122. Johnson, S.S.; Pavlov, A.A.; Mischna, M.A. Fate of SO₂ in the ancient Martian atmosphere: Implications for transient greenhouse warming. *J. Geophys. Res.* **2009**, *114*, E11011.

123. Huang, X.; Gamache, R.R.; Freedman, R.S.; Schwenke, D.W.; Lee, T.J. Reliable infrared line lists for 13 CO₂ isotopologues up to E = 18,000 cm⁻¹ and 1500 K, with line shape parameters. *J. Quant. Spectrosc. Radiat. Transf.* **2014**, *147*, 134–144.
124. Błęcka, M.I.; De Mazière, M. Detection of nitric acid and nitric oxides in the terrestrial atmosphere in the middle-infrared spectral region. *Ann. Geophys.* **1997**, *14*, 1103–1110.
125. Cooper, M.; Martin, R.V.; Sauvage, B.; Boone, C.D.; Walker, K.A.; Bernath, P.F.; McLinden, C.A.; Degenstein, D.A.; Volz-Thomas, A.; Wespes, C. Evaluation of ACE-FTS and OSIRIS Satellite retrievals of ozone and nitric acid in the tropical upper troposphere: Application to ozone production efficiency. *J. Geophys. Res.* **2011**, *116*, D12306.
126. Seager, S.; Bains, W.; Hu, R. A Biomass-based Model to Estimate the Plausibility of Exoplanet Biosignature Gases. *Astrophys. J.* **2013**, *775*, 104.
127. Brown, L.R.; Crisp, J.A.; Crisp, D.; Naumenko, O.V.; Smirnov, M.A.; Sinitza, L.N.; Perrin, A. The Absorption Spectrum of H₂S Between 2150 and 4260 cm⁻¹: Analysis of the Positions and Intensities in the First (2ν₂, ν₁, and ν₃) and Second (3ν₂, ν₁/ν₂, and ν₂/ν₃) Triad Regions. *J. Mol. Spectrosc.* **1998**, *188*, 148–174.
128. Somerville, W.B. Interstellar radio spectrum lines. *Rep. Prog. Phys.* **1977**, *40*, 483–565.
129. Lovas, F.J.; Johnson, D.R.; Snyder, L.E. Recommended rest frequencies for observed interstellar molecular transitions. *Astrophys. J. Suppl.* **1979**, *41*, 451–480.
130. Tomkin, J.; Lambert, D.L. Isotopic abundances of magnesium 5 G-dwarfs and K-dwarfs. *Astrophys. J.* **1980**, *235*, 925–938.
131. McWilliam, A.; Lambert, D.L. Isotopic magnesium abundances in stars. *Mon. Not. R. Astron. Soc.* **1988**, *230*, 573–585.
132. Gay, P.L.; Lambert, D.L. The isotopic abundances of magnesium in stars. *Astrophys. J.* **2000**, *533*, 260–270.
133. Yong, D.; Lambert, D.L.; Ivans, I.I. Magnesium isotopic abundance ratios in cool stars. *Astrophys. J.* **2003**, *599*, 1357–1371.
134. Hinkle, K.H.; Wallace, L.; Ram, R.S.; Bernath, P.F.; Sneden, C.; Lucatello, S. The magnesium isotopologues of MgH in the A²Π – X²Σ⁺ system. *Astrophys. J. Suppl.* **2013**, *207*, 26.
135. GharibNezhad, E.; Shayesteh, A.; Bernath, P.F. Einstein A coefficients for rovibronic lines of the A²Π → X²Σ⁺ and B²Σ⁺ → X²Σ⁺ transitions of MgH. *Mon. Not. R. Astron. Soc.* **2013**, *432*, 2043–2047.
136. Henderson, R.D.E.; Shayesteh, A.; Tao, J.; Haugen, C.C.; Bernath, P.F.; Le Roy, R.J. Accurate Analytic Potential and Born-Oppenheimer Breakdown Functions for MgH and MgD from a Direct-Potential-Fit Data Analysis. *J. Phys. Chem. A* **2013**, *117*, 13373–13387.
137. Reiners, A.; Homeier, D.; Hauschildt, P.H.; Allard, F. A high resolution spectral atlas of brown dwarfs. *Astron. Astrophys.* **2007**, *473*, 245–255.
138. Darby-Lewis, D.; Tennyson, J.; Lawson, K.D.; Yurchenko, S.N.; Stamp, M.F.; Shaw, A.; Brezinsek, S.; JET Contributor. Synthetic spectra of BeH, BeD and BeT for emission modelling in JET plasmas. *J. Phys. B At. Mol. Opt. Phys.* **2018**, submitted.
139. Shanmugavel, R.; Bagare, S.P.; Rajamanickam, N.; Balachandra Kumar, K. Identification of Beryllium Hydride Isotopomer Lines in Sunspot Umbral Spectra. *Serb. Astron. J.* **2008**, *176*, 51–58.
140. Duxbury, G.; Stamp, M.F.; Summers, H.P. Observations and modelling of diatomic molecular spectra from JET. *Plasma Phys. Control. Fusion* **1998**, *40*, 361–370.
141. Wallace, L.; Hinkle, K.; Livingston, W. *An Atlas of Sunspot Umbral Spectra in the Visible from 15,000 to 25,000 cm⁻¹ (3920 to 6664 Å)*; Technical Report Tech. Rep. 00-001; National Solar Observatory: Tucson, AZ, USA, 2000.
142. Kaminski, T.; Wong, K.T.; Schmidt, M.R.; Mueller, H.S.P.; Gottlieb, C.A.; Cherchneff, I.; Menten, K.M.; Keller, D.; Bruenken, S.; Winters, J.M.; et al. An observational study of dust nucleation in Mira (o Ceti) I. Variable features of AlO and other Al-bearing species. *Astron. Astrophys.* **2016**, *592*, A42.
143. Li, G.; Gordon, I.E.; Bernath, P.F.; Rothman, L.S. Direct fit of experimental ro-vibrational intensities to the dipole moment function: Application to {HCl}. *J. Quant. Spectrosc. Radiat. Transf.* **2011**, *112*, 1543–1550.
144. Tenenbaum, E.D.; Woolf, N.J.; Ziurys, L.M. Identification of phosphorus monoxide (X²Π) in VY Canis Majoris: Detection of the first P-O bond in space. *Astrophys. J.* **2007**, *666*, L29–L32.
145. De Beck, E.; Kaminski, T.; Patel, N.A.; Young, K.H.; Gottlieb, C.A.; Menten, K.M.; Decin, L. PO and PN in the wind of the oxygen-rich AGB star IK Tauri. *Astron. Astrophys.* **2013**, *558*, 9.
146. Rivilla, V.M.; Fontani, F.; Beltrán, M.T.; Vasyunin, A.; Caselli, P.; Martín-Pintado, J.; Cesaroni, R. The First Detections of the Key Prebiotic Molecule PO in Star-forming Regions. *Astrophys. J.* **2016**, *826*, 161.

147. Lefloch, B.; Vastel, C.; Viti, S.; Jimenez-Serra, I.; Codella, C.; Podio, L.; Ceccarelli, C.; Mendoza, E.; Lepine, J.R.D.; Bachiller, R. Phosphorus-bearing molecules in solar-type star-forming regions: First PO detection. *Mon. Not. R. Astron. Soc.* **2016**, *462*, 3937.
148. Jones, H.R.A.; Pavlenko, Y.; Viti, S.; Barber, R.J.; Yakovina, L.; Pinfeld, D.; Tennyson, J. Carbon monoxide in low-mass dwarf stars. *Mon. Not. R. Astron. Soc.* **2005**, *358*, 105–112.
149. De Kok, R.J.; Brogi, M.; Snellen, I.A.G.; Birkby, J.; Albrecht, S.; de Mooij, E.J.W. Detection of carbon monoxide in the high-resolution day-side spectrum of the exoplanet HD 189,733b. *Astron. Astrophys.* **2013**, *554*, A82.
150. Brogi, M.; de Kok, R.J.; Birkby, J.L.; Schwarz, H.; Snellen, I.A.G. Carbon monoxide and water vapor in the atmosphere of the non-transiting exoplanet HD 179,949 b. *Astron. Astrophys.* **2014**, *565*, A124.
151. Tennyson, J. Vibration-rotation transition intensities from first principles. *J. Mol. Spectrosc.* **2014**, *298*, 1–6.
152. Danielak, J.; Domin, U.; Kepa, R.; Rytel, M.; Zachwieja, M. Reinvestigation of the emission gamma band system ($A^2\Sigma^+ - X^2\Pi$) of the NO molecule. *J. Mol. Spectrosc.* **1997**, *181*, 394–402.
153. Pavlenko, Y.V. A “lithium test” and modeling of lithium lines in late-type M dwarfs: Teide1. *Astron. Rep.* **1997**, *41*, 537–542.
154. Bittner, D.M.; Bernath, P.F. Line Lists for LiF and LiCl in the $X^1\Sigma^+$ Ground State. *Astrophys. J. Suppl.* **2018**, *235*, 8.
155. McKemmish, L.K.; Yurchenko, S.N.; Tennyson, J. Ab initio calculations to support accurate modelling of the rovibronic spectroscopy calculations of vanadium monoxide (VO). *Mol. Phys.* **2016**, *114*, 3232–3248.
156. Tennyson, J.; Lodi, L.; McKemmish, L.K.; Yurchenko, S.N. The ab initio calculation of spectra of open shell diatomic molecules. *J. Phys. B At. Mol. Opt. Phys.* **2016**, *49*, 102001.
157. Cushing, M.C.; Rayner, J.T.; Davis, S.P.; Vacca, W.D. FeH absorption in the near-infrared spectra of late M and L dwarfs. *Astrophys. J.* **2003**, *582*, 1066–1072.
158. Hargreaves, R.J.; Hinkle, K.H.; Bauschlicher, C.W., Jr.; Wende, S.; Seifahrt, A.; Bernath, P.F. High-resolution 1.6 μm spectra of FeH in M and L dwarfs. *Astron. J.* **2010**, *140*, 919–924.
159. Wallace, L.; Hinkle, K. Detection of the 1.6 μm $E^4\Pi - A^4\Pi$ FeH system in sunspot and cool star spectra. *Astrophys. J.* **2001**, *559*, 424–427.
160. Ramos, A.A.; Bueno, J.T.; Collados, M. Detection of polarization from the $E^4\Pi - A^4\Pi$ system of FeH in sunspot spectra. *Astrophys. J.* **2004**, *603*, L125–L128.
161. Harrison, J.J.; Brown, J.M. Measurement of the magnetic properties of FeH in its $X^4\Delta$ and $F^4\Delta$ states from sunspot spectra. *Astrophys. J.* **2008**, *686*, 1426–1431.
162. DeYonker, N.J.; Allen, W.D. Taming the low-lying electronic states of FeH. *J. Chem. Phys.* **2012**, *137*, 234303.
163. Dulick, M.; Bauschlicher, C.W.; Burrows, A.; Sharp, C.M.; Ram, R.S.; Bernath, P. Line intensities and molecular opacities of the FeH $F^4\Delta - X^4\Delta$ transition. *Astrophys. J.* **2003**, *594*, 651–663.
164. Rajpurohit, A.S.; Reyle, C.; Allard, F.; Homeier, D.; Schultheis, M.; Bessell, M.S.; Robin, A.C. The effective temperature scale of M dwarfs. *Astron. Astrophys.* **2013**, *556*, A15.
165. Ardila, D.R.; Van Dyk, S.D.; Makowiecki, W.; Stauffer, J.; Song, I.; Rho, J.; Fajardo-Acosta, S.; Hoard, D.W.; Wachter, S. The Spitzer atlas of stellar spectra (SASS). *Astrophys. J. Suppl.* **2010**, *191*, 301–339.
166. Campbell, J.M.; Klapstein, D.; Dulick, M.; Bernath, P.F. Infrared-absorption and emission-spectra of SiO. *Astrophys. J. Suppl.* **1995**, *101*, 237–254.
167. Wallace, L.; Hinkle, K. Medium-resolution stellar spectra in the L band from 2400 to 3000 cm^{-1} (3.3 to 4.2 microns). *Astron. J.* **2002**, *124*, 3393–3399.
168. Joshi, G.C.; Punetha, L.M.; Pande, M.C. (A–X) system of SiO in sunspots. *Sol. Phys.* **1979**, *62*, 77–82.
169. Bauschlicher, C.W., Jr. The low-lying electronic states of SiO. *Chem. Phys. Lett.* **2016**, *658*, 76–79.
170. Kurucz, R.L. Including all the lines. *Can. J. Phys.* **2011**, *89*, 417–428.
171. Bai, X.; Motto-Ros, V.; Lei, W.; Zheng, L.; Yu, J. Experimental determination of the temperature range of AlO molecular emission in laser-induced aluminum plasma in air. *Spectra Chim. Acta B* **2014**, *99*, 193–200.
172. Surmick, D.M.; Parigger, C.G. Aluminum Monoxide Emission Measurements in a Laser-Induced Plasma. *Appl. Spectrosc.* **2014**, *68*, 992–996.
173. Parigger, C.G.; Hornkohl, J.O. Computation of AlO $B^2\Sigma^+ \rightarrow X^2\Sigma^+$ emission spectra. *Spectra Chim. Acta A* **2011**, *81*, 404–411.
174. Kirkpatrick, J.D.; Kelly, D.M.; Rieke, G.H.; Liebert, J.; Allard, F.; Wehrse, R. M dwarf spectra from 0.6 to 1.5 micron-A spectral sequence, model atmosphere fitting, and the temperature scale. *Astrophys. J.* **1993**, *402*, 643–654.

175. McGovern, M.R.; Kirkpatrick, J.D.; McLean, I.S.; Burgasser, A.J.; Prato, L.; Lowrance, P.J. Identifying Young Brown Dwarfs Using Gravity-Sensitive Spectral Features. *Astrophys. J.* **2004**, *600*, 1020.
176. Kirkpatrick, J.D.; Barman, T.S.; Burgasser, A.J.; McGovern, M.R.; McLean, I.S.; Tinney, C.G.; Lowrance, P.J. Discovery of a Very Young Field L Dwarf, 2MASS J01415823–4633574. *Astrophys. J.* **2006**, *639*, 1120.
177. Peterson, D.E.; Megeath, S.T.; Luhman, K.L.; Pipher, J.L.; Stauffer, J.R.; Barrado y Navascués, D.; Wilson, J.C.; Skrutskie, M.F.; Nelson, M.J.; Smith, J.D. New Young Brown Dwarfs in the Orion Molecular Cloud 2/3 Region. *Astrophys. J.* **2008**, *685*, 313.
178. Desert, J.M.; Vidal-Madjar, A.; des Etangs, A.L.; Sing, D.; Ehrenreich, D.; Hebrard, G.; Ferlet, R. TiO and VO broad band absorption features in the optical spectrum of the atmosphere of the hot-Jupiter HD 209458b. *Astron. Astrophys.* **2008**, *492*, 585–592.
179. Allard, F.; Hauschildt, P.H.; Schwenke, D. TiO and H₂O absorption lines in cool stellar atmospheres. *Astrophys. J.* **2000**, *540*, 1005–1015.
180. Sedaghati, E.; Boffin, H.M.J.; MacDonald, R.J.; Gandhi, S.; Madhusudhan, N.; Gibson, N.P.; Oshagh, M.; Claret, A.; Rauer, H. Detection of titanium oxide in the atmosphere of a hot Jupiter. *Nature* **2017**, *549*, 238.
181. Nugroho, S.K.; Kawahara, H.; Masuda, K.; Hirano, T.; Kotani, T.; Tajitsu, A. High-resolution Spectroscopic Detection of TiO and a Stratosphere in the Day-side of WASP-33b. *Astrophys. J.* **2017**, *154*, 221.
182. Tsiaras, A.; Waldmann, I.P.; Zingales, T.; Rocchetto, M.; Morello, G.; Damiano, M.; Karpouzas, K.; Tinetti, G.; McKemmish, L.K.; Tennyson, J.; et al. A Population Study of Gaseous Exoplanets. *Astron. J.* **2018**, *155*, 156.
183. Ryabchikova, T.; Piskunov, N.; Kurucz, R.L.; Stempels, H.C.; Heiter, U.; Pakhomov, Y.; Barklem, P.S. A major upgrade of the VALD database. *Phys. Scr.* **2015**, *90*, 054005.
184. McKemmish, L.K.; Masseron, T.; Yurchenko, S.N.; Tennyson, J. ExoMol Molecular line lists—XXXIV. The spectrum of Titanium Oxide. *Mon. Not. R. Astron. Soc.* **2018**, to be submitted.
185. Wollaston, W.H. A Method of Examining Refractive and Dispersive Powers, by Prismatic Reflection. *Philos. Trans. R. Soc. Lond.* **1802**, *92*, 365–380.
186. Swan, W. On the Prismatic Spectra of the Flames of Compounds of Carbon and Hydrogen. *Trans. R. Soc. Edinb.* **1857**, *21*, 411.
187. Brooke, J.S.; Bernath, P.F.; Schmidt, T.W.; Bacskay, G.B. Line strengths and updated molecular constants for the C₂ Swan system. *J. Quant. Spectrosc. Radiat. Transf.* **2013**, *124*, 11–20.
188. Pavanello, M.; Adamowicz, L.; Aljiah, A.; Zobov, N.F.; Mizus, I.I.; Polyansky, O.L.; Tennyson, J.; Szidarovszky, T.; Császár, A.G.; Berg, M.; et al. Precision measurements and computations of transition energies in rotationally cold triatomic hydrogen ions up to the mid-visible spectral range. *Phys. Rev. Lett.* **2012**, *108*, 023002.
189. Miller, S.; Tennyson, J. Calculated rotational and ro-vibrational transitions in the spectrum of H₃⁺. *Astrophys. J.* **1988**, *335*, 486–490.
190. Miller, S.; Achilleos, N.; Ballester, G.E.; Geballe, T.R.; Joseph, R.D.; Prange, R.; Rego, D.; Stallard, T.; Tennyson, J.; Trafton, L.M.; et al. The role of H₃⁺ in planetary atmospheres. *Philos. Trans. R. Soc. Lond. A* **2000**, *358*, 2485–2502.
191. Shkolnik, E.; Gaidos, E.; Moskovitz, N. No Detectable H₃⁺ Emission from the Atmospheres of Hot Jupiters. *Astrophys. J.* **2006**, *132*, 1267.
192. Koskinen, T.T.; Aylward, A.D.; Miller, S. A stability limit for the atmospheres of giant extrasolar planets. *Nature* **2007**, *450*, 845–848.
193. Miller, S.; Stallard, T.; Melin, H.; Tennyson, J. H₃⁺ cooling in planetary atmospheres. *Faraday Discuss.* **2010**, *147*, 283–291.
194. Miller, S.; Stallard, T.; Tennyson, J.; Melin, H. Cooling by H₃⁺ emission. *J. Phys. Chem. A* **2013**, *117*, 9770–9777.
195. Bergeron, P.; Ruiz, M.T.; Leggett, S.K. The chemical evolution of cool white dwarfs and the age of the local galactic disk. *Astrophys. J. Suppl.* **1997**, *108*, 339–387.
196. Neale, L.; Tennyson, J. A high temperature partition function for H₃⁺. *Astrophys. J.* **1995**, *454*, L169–L173.
197. Sochi, T.; Tennyson, J. A computed line list for the H₂D⁺ molecular ion. *Mon. Not. R. Astron. Soc.* **2010**, *405*, 2345–2350.
198. Herman, M.; Campargue, A.; El Idrissi, M.I.; Vander Auwera, J. Vibrational spectroscopic database on acetylene, X¹Σ_g⁺ (¹²C₂H₂, ¹²C₂D₂ and ¹³C₂H₂). *J. Phys. Chem. Ref. Data* **2003**, *32*, 921–1361.
199. Herman, M. The acetylene ground state saga. *Mol. Phys.* **2007**, *105*, 2217–2241.
200. Jørgensen, U.G.; Almlöf, J.; Siegbahn, P.E.M. Complete active space self-consistent field calculations of the vibrational band strengths for C₃. *Astrophys. J.* **1989**, *343*, 554.

201. Gorman, M.; Yurchenko, S.N.; Tennyson, J. ExoMol Molecular linelists—XXXIII. The spectrum of Chromium Hydride. *Mon. Not. R. Astron. Soc.* **2018**, to be submitted.
202. Gorman, M.; Yurchenko, S.N.; Tennyson, J. ExoMol Molecular linelists—XXXV. The spectrum of manganese hydride. *Mon. Not. R. Astron. Soc.* **2018**, to be submitted.
203. Faure, A.; Wiesenfeld, L.; Tennyson, J.; Drouin, B.J. Pressure broadening of water and carbon monoxide transitions by molecular hydrogen at high temperatures. *J. Quant. Spectrosc. Radiat. Transf.* **2013**, *116*, 79–86.
204. Renaud, C.L.; Cleghorn, K.; Hartmann, L.; Vispoel, B.; Gamache, R.R. Line shape parameters for the H₂O–H₂ collision system for application to exoplanet and planetary atmospheres. *Icarus* **2018**, *306*, 275–284.
205. Barton, E.J.; Hill, C.; Czurylo, M.; Li, H.Y.; Hyslop, A.; Yurchenko, S.N.; Tennyson, J. The ExoMol diet of line-by-line pressure-broadening parameters. *J. Quant. Spectrosc. Radiat. Transf.* **2017**, *203*, 490–495.



© 2018 by the authors. Licensee MDPI, Basel, Switzerland. This article is an open access article distributed under the terms and conditions of the Creative Commons Attribution (CC BY) license (<http://creativecommons.org/licenses/by/4.0/>).